

**ATTEMPTS TO CREATE α -SYNUCLEIN PHOSPHORYLATION
MUTANT CONSTRUCTS USING SITE-DIRECTED MUTAGENESIS
AND TO CREATE γ -SYNUCLEIN GENE SILENCING CONSTRUCTS
USING shRNA CLONING METHOD**

By

LEE YI HENG

A project report submitted to the Department of Biomedical Science

Faculty of Science

Universiti Tunku Abdul Rahman

in partial fulfillment of the requirements for the degree of

Bachelor of Science (Hons) Biomedical Science

May 2013

ABSTRACT

ATTEMPTS TO CREATE α -SYNUCLEIN PHOSPHORYLATION MUTANT CONSTRUCTS USING SITE-DIRECTED MUTAGENESIS AND TO CREATE γ -SYNUCLEIN GENE SILENCING CONSTRUCTS USING shRNA CLONING METHOD

Lee Yi Heng

α -synuclein (α -syn) and γ -synuclein (γ -syn) belong to synuclein protein family which had been implicated in neurodegenerative diseases and cancers. This study aimed to create four α -syn phosphorylation mutant constructs (S87A, S87D, S129A and S129D) using *in vitro* site-directed mutagenesis (SDM) which employs complementary mutagenic primer pairs in whole-plasmid amplification. Competency of self-prepared chemical competent cells used in this study achieved 2.417×10^6 cfu/ μ g plasmid. SDM was originally carried out using Stratagene QuickChange™ Site-Directed Mutagenesis Protocol (QCM) method. However, all the mutagenesis attempts using QCM method were unsuccessful which could be due to low or no amplification. To reduce primer dimer formation, mutagenesis using Single Primer Reaction in Parallel (SPRINP) method which has two separate PCR reactions containing either forward or reverse primers carried out in parallel was performed. However, these attempts also failed to generate desired mutant constructs which could also be due to low or no amplification. Besides, this study also attempted to create three γ -syn gene silencing constructs by cloning the annealed shRNA

oligonucleotides into the dual-digested instability-prone lentiviral plasmid pLKO.1 TRC. However, subsequent transformations of ligation products into self-prepared competent *E. coli* DH5 α and JM109 recovered plasmids which gave unexpected bands pattern when insert screening was performed using restriction enzyme digestion. This could be suggestive of plasmid instability and switching over to another cloning host that could provide better plasmid stability may be needed.

ACKNOWLEDGEMENTS

Throughout the course of the project, I received the help from many people. I would like to express my utmost appreciation to my project supervisor, Dr. Say Yee How for his patience in guiding me to complete the laboratory works and thesis writing. My appreciation also goes to lab mates, postgraduates, lab officers and Faculty of Science, UTAR. Last but not least, I would like to express my gratitude to my family members for their tremendous support.

DECLARATION

I hereby declare that the project report is based on my original work except for quotations and citations which have been duly acknowledged. I also declare that it has not been previously or concurrently submitted for any other degree at Universiti Tunku Abdul Rahman or other institutions.

.....

LEE YI HENG

APPROVAL SHEET

This project report entitled **“ATTEMPTS TO CREATE α -SYNUCLEIN PHOSPHORYLATION MUTANT CONSTRUCTS USING SITE-DIRECTED MUTAGENESIS AND TO CREATE γ -SYNUCLEIN GENE SILENCING CONSTRUCTS USING shRNA CLONING METHOD”**

was prepared by **LEE YI HENG** and submitted as partial fulfillment of the requirements for the degree of Bachelor of Science (Hons) Biomedical Science at Universiti Tunku Abdul Rahman.

Approved by,

.....

(Dr. Say Yee How)

Supervisor

Department of Biomedical Science

Faculty of Science,

Universiti Tunku Abdul Rahman

Date:

UNIVERSITI TUNKU ABDUL RAHMAN

FACULTY OF SCIENCE

Date: _____

PERMISSION SHEET

It is hereby certified that **LEE YI HENG** (ID No: **09ADB06938**) has completed this final year project entitled “*Attempts to Create α -synuclein Phosphorylation Mutant Constructs using Site-directed Mutagenesis and to Create γ -synuclein Gene Silencing Constructs using shRNA Cloning Method*” under the supervision of Dr. Say Yee How from the Department of Biomedical Science, Faculty of Science.

I understand that University will upload softcopy of my final year project in pdf format into UTAR Institutional Repository, which may be made accessible to UTAR community and public.

Yours truly,

(Lee Yi Heng)

TABLE OF CONTENTS

	PAGE
ABSTRACT	ii
ACKNOWLEDGEMENT	iv
DECLARATION	v
APPROVAL SHEET	vi
PERMISSION SHEET	vii
TABLE OF CONTENTS	viii
LIST OF TABLES	xii
LIST OF FIGURES	xiv
LIST OF ABBREVIATIONS	xvi

CHAPTER

1.0 INTRODUCTION	1
2.0 LITERATURE REVIEW	5
2.1 Family of Synucleins	5
2.2 α -syn	6
2.2.1 α -synucleinopathy and Parkinson's Disease	6
2.2.2 Biochemistry and Structure of α -syn	7
2.2.3 Functions and Behaviors of α -syn	10
2.2.4 Phosphorylation of α -syn	11
2.3 γ -syn	15
2.3.1 Structure, Properties and Functions of γ -syn	15
2.3.2 Association of γ -syn with Neurodegenerative Diseases	16
2.3.3 Association of γ -syn with Cancers	17

2.4	<i>In vitro</i> Site-directed Mutagenesis	18
2.5	RNA interference (RNAi)	22
3.0	MATERIALS AND METHODS	25
3.1	List of Materials and Apparatus	25
3.2	Molecular Biology of α -syn Phosphorylation Mutant Constructs	29
3.2.1	Mammalian Expression Vector, pcDNA TM 3.1D/V5-His-TOPO with Full Length Wild Type Human α -syn	29
3.2.2	Primer Design for Generation of α -syn Phosphorylation Mutant Constructs	30
3.3	Preparation of Chemical Competent Cells	31
3.4	Cell Competency Test	32
3.4.1	Heat Shock Transformation	32
3.4.2	Serial Dilution	33
3.5	Propagation of Plasmid Template in <i>dam</i> ⁺ <i>dcm</i> ⁺ <i>E. coli</i>	33
3.5.1	Transformation and Plasmid Extraction (Midipreparation)	33
3.5.2	Linearization of Plasmid	34
3.6	Mutant Strand Synthesis	35
3.6.1	Stratagene QuickChange TM Site-directed Mutagenesis Protocol	35
3.6.2	Single Primer Reaction in Parallel	36
3.6.3	Plasmid Extraction (Minipreparation), Linearization and Sequencing	38
3.7	Molecular Biology of γ -syn Gene Silencing Constructs	38
3.7.1	Lentiviral Plasmid pLKO.1 TRC	38

3.7.2	Design of shRNA Oligonucleotides against Human γ -syn Gene	40
3.7.3	Annealing of shRNA Oligonucleotides	43
3.7.4	Dual Digestion of Lentiviral Plasmid pLKO.1 TRC	43
3.7.5	Ligation and Transformation into Competent Cells	44
3.7.6	Plasmid Extraction, Screening of shRNA Inserts and Sequencing	46
4.0	RESULTS	47
4.1	Competency Test for Self-prepared Chemical Competent Cells	47
4.2	Propagation of Plasmid Template in <i>dam</i> ⁺ <i>dcm</i> ⁺ <i>E. coli</i>	48
4.2.1	Plasmid Extraction (Midipreparation)	48
4.2.2	Confirmation of Purified Plasmid using <i>Xho</i> I Linearization	49
4.3	Mutant Strand Synthesis	50
4.3.1	Transformation and Plasmid Extraction (Minipreparation)	50
4.3.2	Screening using <i>Xho</i> I Linearization and Sequencing	53
4.3.3	Troubleshooting	57
4.4	Generation of γ -syn Gene Silencing Constructs	60
4.4.1	Dual Digestion of Lentiviral Plasmid pLKO.1 TRC	60
4.4.2	Efficiency of shRNA Oligonucleotides Annealing	62
4.4.3	Gel Analysis of Ligation Products	63
4.4.4	Transformation of Ligation Products and Plasmid Extraction	65

4.4.5	Screening of shRNA Inserts and Sequencing	66
5.0	DISCUSSION	68
5.1	Generation of α -syn Phosphorylation Mutant Constructs	68
5.1.1	Competent Cells	68
5.1.2	Propagation of Plasmid Template in <i>dam⁺ dcm⁺ E. coli</i>	70
5.1.3	Inefficient Mutant Strand Synthesis	71
5.1.4	Incomplete <i>DpnI</i> Selection	74
5.1.5	Future Studies	75
5.2	Generation of γ -syn Gene Silencing Constructs	77
5.2.1	Dual Digestion of Lentiviral Plasmid pLKO.1 TRC	77
5.2.2	Suboptimal Efficiency of shRNA Oligonucleotides Annealing	78
5.2.3	Plasmid Instability	79
5.2.4	Future Studies	82
6.0	CONCLUSIONS	84
	REFERENCES	85
	APPENDICES	97

LIST OF TABLES

Table		Page
3.1	List of apparatus and equipment used for this study and their respective manufacturers	25
3.2	List of material used for this study and their respective manufacturers	26
3.3	List of solutions used for this study and their respective formulation.	28
3.4	Forward (F) and reverse (R) primers used for generation of α -syn phosphorylation mutant constructs and their respective sequences.	31
3.5	Composition of PCR reaction (QCM) used for α -syn phosphorylation mutant constructs (S87A, S87D, S129A and S129D).	36
3.6	Composition of PCR reaction (SPRINP) used for α -syn phosphorylation mutant constructs (S87A, S87D, S129A and S129D).	37
3.7	List of 21-mer target sequences in <i>SNCG</i> gene for efficient gene silencing.	41
3.8	Forward and reverse oligonucleotides for the three γ -syn shRNA constructs.	42
3.9	Preparation of mixture for annealing of shRNA oligonucleotides.	43
3.10	Reaction mixture for simultaneous dual digestion of lentiviral plasmid pLKO.1 using <i>Age</i> I and <i>Eco</i> RI.	44
3.11	Ligation mixture for cloning of annealed oligonucleotides into lentiviral plasmid pLKO.1 in generation of shRNA constructs.	45
4.1	Nano-spectrophotometry analysis showing A_{260} , A_{280} , purity and concentration of the purified plasmid DNA (midpreparation).	49

4.2	Number of colonies, screened colonies and mutant obtained using Stratagenes QuickChange TM Site-Directed Mutagenesis Protocol (QCM) with DH5 α as the transformation host.	51
4.3	Number of colonies, screened colonies and mutant obtained using Single Primer Reaction in Parallel (SPRINP) with DH5 α as the transformation host.	52
4.4	Number of colonies, screened colonies and mutant obtained using Single Primer Reaction in Parallel (SPRINP) with JM109 as the transformation host.	52
4.5	Nano-spectrophotometry analysis showing the A ₂₆₀ , A ₂₈₀ , purity and concentration of plasmid (Clone 1, Clone 2 and Clone) purified from transformed colonies for γ -syn shRNA 3.	65

LIST OF FIGURES

Figure		Page
2.1	Organization of human synuclein genes (<i>SCNA</i> , <i>SCNB</i> and <i>SCNG</i>).	6
2.2	α -syn tetramer.	8
2.3	Molecular structure of α -syn.	9
2.4	Schematic diagram of Stratagene QuickChange TM Site-Directed Mutagenesis Protocol (QCM).	20
2.5	Schematic diagram of RNAi pathway.	23
3.1	Map of pcDNA TM 3.1D/ V5-His-TOPO vector.	30
3.2	Map of lentiviral plasmid pLKO.1 TRC containing a shRNA insert.	39
3.3	Main elements of shRNA complementary oligonucleotides include sense sequence, spacer or loop region and antisense sequence.	42
4.1	Self-prepared chemical competent <i>E. coli</i> DH5 α transformed with pcDNA TM 3.1D/V5-His-TOPO WT α -syn on LB ampicillin agar plate.	47
4.2	Electrophoresis gel (1% agarose) image showing migration of linearized and unlinearized purified plasmid (Midipreparation).	50
4.3	Electrophoresis gel (1% agarose) image showing the screening of purified plasmid (minipreparation) using <i>Xho</i> I linearization before sequencing.	54
4.4	Sequencing chromatogram of purified plasmid (minipreparation) in S87D mutant construction.	55
4.5	Sequence alignment between purified plasmid (minpreparation) for S87A and S87D mutant constructions and full-length wild type human α -syn (GenBank ID: BC108275.1) cDNA (Clone ID: 6147966).	56

4.6	Sequencing chromatogram of purified plasmid (minipreparation) in S129D mutant construction.	56
4.7	Sequence alignment between purified plasmid (minipreparation) for S129A and S129D mutant constructions and full-length wild type human α -syn (GenBank ID: BC108275.1) cDNA (Clone ID: 6147966).	57
4.8	Electrophoresis gel (1% agarose) image showing migration of post- <i>DpnI</i> -treated PCR (QCM) products.	58
4.9	Electrophoresis gel (1% agarose) image showing migration of post- <i>DpnI</i> -treated PCR (SPRINP) products.	59
4.10	Electrophoresis gel (1% agarose) image showing migration of gel purification product for non-stuffer pLKO.1 TRC.	61
4.11	Electrophoresis gel (3% agarose) image showing the annealing efficiency test of shRNA oligonucleotides.	63
4.12	Electrophoresis gel (1% agarose) image showing migration of ligation products and non-stuffer pLKO.1 TRC.	64
4.13	Electrophoresis gel (1% agarose) image showing migration of unlinearized purified plasmid and the respective dual digested products in the screening of shRNA insert for γ -syn shRNA 3.	67

LIST OF ABBREVIATIONS

α -syn	α -synuclein
β -syn	β -synuclein
γ -syn	γ -synuclein
BSA	Bovine Serum Albumin
DMSO	Dimethyl Sulphoxide
EDTA	Ethylenediaminetetraacetic acid
LB	Luria Bertani
pcDNA TM 3.1D/V5-His-TOPO WT α -syn	pcDNA TM 3.1D/V5-His-TOPO cloned with full-length wild type human α -syn (GenBank ID: BC108275.1) cDNA (Clone ID: 6147966)
PCR	Polymerase Chain Reaction
PD	Parkinson's Disease
QCM	QuickChange TM Site-Directed Mutagenesis Protocol
shRNA	Small Hairpin RNA
SDM	Site-directed Mutagenesis
SPRINP	Single Primer Reaction in Parallel
TE	Tris-EDTA
TRC	The RNAi Consortium

CHAPTER 1

INTRODUCTION

Synuclein is a group of small and soluble neuronal proteins including α -, β - and γ -syn that share high sequence homology. They are found in vertebrates but not in invertebrates (George 2001). To date, their function are basically still unclear, however, their implication in neurodegenerative diseases and cancers may provide insights into underlining pathomechanisms leading to these two groups of diseases, and may possibly be explored as therapeutic targets for these debilitating diseases.

Parkinson's disease (PD) as the most common neurodegenerative disease besides Alzheimer's disease (Guttmacher and Collins 2003) is characterized by selective loss of dopaminergic neurons in the substantia nigra pars compacta as well as the presence of cytoplasmic eosinophilic inclusion known as Lewy body. α -Syn is known to play a central role in the pathogenesis of PD. This could be attributed to the two evidences, including three rare missense mutations (A53T, A30P and E46K) in α -syn which are associated with autosomal dominant PD in some families as well as their presence as the major component of Lewy bodies and Lewy neurites in both familial PD and sporadic PD patients (Okochi et al., 2000; Saha et al., 2003; Kruger 2004; Chau et al., 2009; Sato et al., 2011).

Many studies showed that the α -syn present in the brain of PD patients is highly phosphorylated (Valtierra 2008). Findings that phosphorylation occurs dominantly at S129 (Fujiwara et al., 2002; Anderson et al., 2006) and less dominantly at S87 (Okochi et al., 2000) of α -syn found in Lewy bodies have linked phosphorylation of α -syn at these two sites to the formation of Lewy bodies and PD pathogenesis.

Serine is a hydrophilic amino acid with hydroxyl group at its side chain. It is uncharged polar amino acid and is usually phosphorylated within intracellular environment (Betts and Russel 2003). Studies involving the effect and function of phosphorylation always utilize the phosphomimic and phospho-dead mutant construct. Effect of phosphorylation could be mimicked by introducing negatively charged residues like aspartate and glutamic acid (Leger et al., 1997). Glutamate and aspartate have high structural similarity with phosphoserine and phosphothreonine and thus are usually used as phosphomimetic of these residues. Conversely, the abolishment of phosphorylation (phospho-dead mutant) could be modelled by introducing the uncharged amino acid alanine. This opposes the phosphate group which carries charge. Hence, site-directed mutagenesis could be used to replace the serine residues at both codon 87 and 129 of α -syn with aspartate residue and alanine residue to generate α -syn phosphorylation mutant constructs (S87A, S87D, S129A and S129D).

γ -syn is the third member of the synuclein family which is believed to be implicated in pathogenesis of cancers and neurodegenerative diseases (Ahmah

et al., 2007). Similar to other members of the family, the physiological functions of γ -syn within the cell remain elusive (Shen et al., 2011).

γ -syn is well implicated in the process of tumorigenesis and metastasis. It was originally discovered as *BCSG1* (Breast Cancer Specific Gene 1) and was found to be expressed according to the stages of cancer (Ji et al., 1997; Wu et al., 2003). Implication of γ -syn in neurodegenerative diseases is less established. γ -Syn has been implicated in glaucoma pathology (Surgucheva et al., 2002) but the underlining mechanism remains elusive. It also involves in axonal pathology near the hippocampal region of the PD brains (Galvin et al., 1999).

Gene silencing of γ -syn in prostate cancer cell line (Chen et al., 2012) and gall bladder cancer cell line (Han et al., 2012) inhibited their tumorigenic and metastatic activities, further suggesting involvement of γ -syn in tumorigenesis. These findings also shed light of possible therapeutic approach for metastatic cancer by using gene silencing of γ -syn. Recent study made by Surgucheva et al. (2012) has shown that γ -syn could induce the aggregation of α -syn. Since α -syn aggregation (Braithwaite et al., 2012) has been associated with PD, this finding also sheds light of possible therapeutic approach for PD by using gene silencing of γ -syn.

Therefore, the objectives of this study were:

1. To prepare competent cells with competency met the range sufficient for routine cloning experiment using chemical method.
2. To generate α -syn phosphorylation mutant constructs (S87A, S87D, S129A and S129D) using site-directed mutagenesis which include thermal cycling for whole-plasmid amplification, *DpnI* selection and subsequent recovery of mutant constructs through transformation into self-prepared chemical competent cells.
3. To generate γ -syn shRNA constructs via cloning of annealed shRNA oligonucleotides into dual-digested lentiviral plasmid and subsequent recovery of the constructs through transformation into self-prepared chemical competent cells.

CHAPTER 2

LITERATURE REVIEW

2.1 Family of Synucleins

Synuclein family comprises of three small, acidic and soluble neuronal protein members, which are α -, β - and γ -syn. All these three members share a conserved N-terminal domain that is characterized by 5-6 repeats of the KTKEGV consensus sequence in the first 87 residues (Jakes et al., 1994). There is higher expression of these three proteins in brain region compared with other organs like heart, skeletal muscles and liver (Lavedan 1998). α - and β -syn are expressed primarily in brain tissues (George 2001) whereas γ -syn are expressed in peripheral nervous system including sensory neurons, brain and some tumors including breast cancer and ovarian tumor (Ji et al., 1997; Bruening et al., 2000)

The *SNCA*, *SNCB* and *SNCG* genes which encode for α -syn, β -syn and γ -syn respectively in human have been mapped to chromosome 4q21.3-q22 (Chen et al., 1995), 5q35 (Spillantini et al., 1995), and 10q23 (Ninkina et al., 1998) respectively. The *SCNA* gene consists of seven exons, five of which are protein-coding. *SCNB* gene consists of six exons, five of which are protein-coding while the *SCNG* gene consists of five exons in which all the exons are protein-coding (George 2001) (Figure 2.1). Although the calculated molecular mass of synucleins is close to 14 kDa, the exact molecular mass is

approximately 19-20 kDa in which this suggests the occurrence of post-translational modification (Jakes et al., 1994).

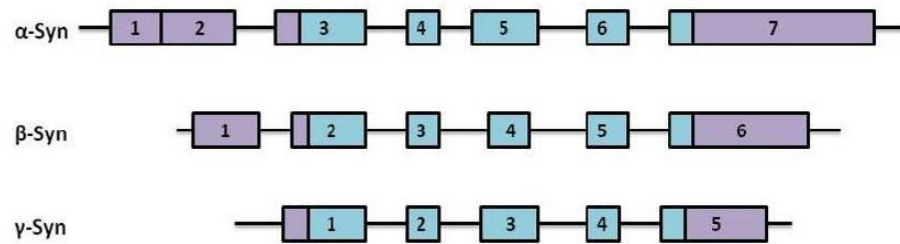


Figure 2.1: Organization of human synuclein genes (*SCNA*, *SCNB* and *SCNG*). Blue and purple boxes represent the protein-coding region and untranslated regions of the exons respectively. The interrupted horizontal lines represent the introns of the genes (Choong 2011).

2.2 α-syn

2.2.1 α-synucleinopathy and Parkinson's Disease

α-synucleinopathy is a group of diseases which is characterized by abnormal aggregation of α-syn in affected brain regions. These include PD (Baba et al., 1998), multiple system atrophy (MSA) (Tong et al., 2010), dementia with Lewy bodies (DLB) (Kramer and Schulz-Schaeffer 2007), neurodegeneration with brain iron accumulation type 1 (NBIA-1; previously known as Hallervorden-Spatz syndrome) (Neumann et al., 2000), amyotrophic lateral sclerosis (ALS) (Kokubo et al., 2012) and Lewy body variant of Alzheimer's disease (AD) (Mukaetova-Ladinska et al., 2009).

The pathological hallmarks of PD include the presence of Lewy bodies and the loss of dopaminergic neurons in substantial nigra particularly the ventral component of pars compacta. Usually, there is a loss of 50% to 70% of neuron in this particular brain region of the dead patient due to PD compared to the same brain region of unaffected individual (Davie 2008). The progression of disease could be staged according to the topographic location of Lewy body pathology in brain. In stages 1-2 which are presymptomatic stages, inclusion body pathology is found only in medulla oblongata, pontine tegmentum and olfactory bulb. In stages 3-4 where PD patients may start to exhibit certain clinical motor symptoms like bradykinesia, rigidity and tremor, substantial nigra and nuclear grays of the midbrain and forebrain are involved. In the final stages 5-6 where cognitive impairment might occurs, neocortex is involved (Braak et al., 2003; Braak et al., 2004).

2.2.2 Biochemistry and Structure of α -syn

α -syn has long been described as natively unfolded monomeric protein which does not possess defined structure in aqueous solution (Stefanis 2012). However, recent study showed that α -syn isolated from neuronal and non-neuronal cell line exists as tetramer form physiologically rather than previously-thought monomeric form. Previous concept of monomeric α -syn was derived from the studies using recombinant protein expressed in bacteria which may explain the structural difference (Bartels et al., 2011). The α -syn tetramer of about 58 kDa (Figure 2.2) also appeared to resist aggregation in which this suggests that destabilization and disruption of tetramer into

monomer may be needed before misfold and aggregation of α -syn as happen in PD (Bartels et al., 2011).

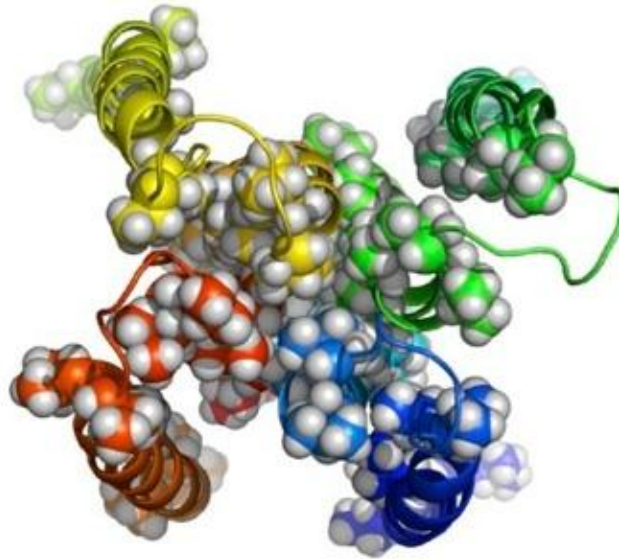


Figure 2.2: α -syn tetramer. This proposed structure is based on electron microscopy (EM) reconstruction and paramagnetic relaxation enhancement (PRE) (Pochapsky 2012).

α -syn with molecular weight of 19 kDa comprises of 140 amino acid residues. There are three distinct regions that make up the proteins, which are N-terminal amphipathic region (residues 1-65), central hydrophobic region or hydrophobic non-amyloid component (NAC) (residues 66-95) and C-terminal acidic region (residues 96-140) (Clayton and George 1998; Cheng et al., 2010) (Figure 2.3). N-terminal half of the α -syn that covers both N-terminal amphipathic region and central hydrophobic region consists of seven imperfect 11-mer repeats with a consensus 6-residues motif KTKEGV. The

11-mer repeat forms the conserved apolipoprotein-like class-A2 helix which is essential in mediating reversible α -syn-lipid interaction (Davidson et al., 1998; Bussell and Eliezer 2003).

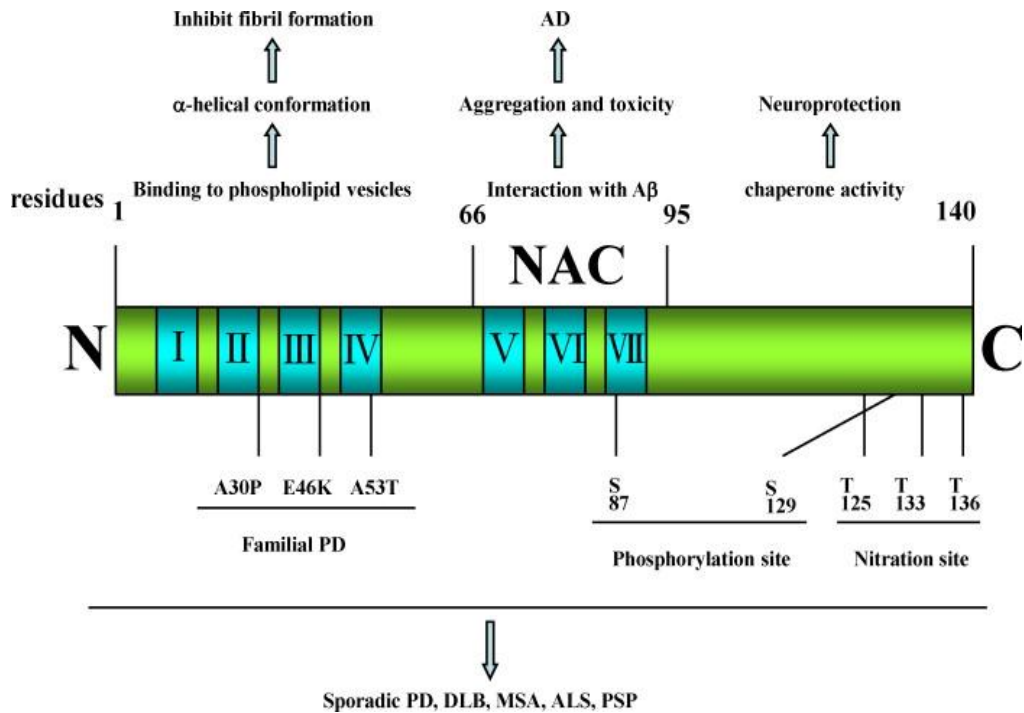


Figure 2.3: Molecular structure of α -syn. α -syn protein could be subdivided into three regions including N-terminal region (residues 1-65), central hydrophobic region or NAC (residues 66-95) and C-terminal region (residues 96-140). Four of the seven imperfect 11-mer repeats with conserved KTKEGV motifs (blue color) are distributed in N-terminal region. Note that codon S87 is located in NAC while codon S129 is located in C-terminal region (Cheng et al., 2010).

N-terminal amphipathic region is implicated in membrane binding activity of α -syn via the formation of α helical structure (Stefanis 2012). Central hydrophobic region or NAC which distinguishes α -syn from β -syn, appeared to be responsible for β -sheet form of protein and subsequent aggregation

(Jakes et al., 1994). The C-terminal region may play a role in preventing aggregation (Crowther et al., 1998; Li et al., 2005), chaperone activity (Kim et al., 2002) and protection against oxidative stress (Kanda et al., 2000; Albani et al., 2004).

2.2.3 Functions and Behaviors of α -syn

The function of α -syn remains elusive although a lot of research have been done to understand it. To date, α -syn is ascribed to play roles in synaptic physiology due to the evidences that show that α -syn is predominantly localized to presynaptic terminal (Kahle 2008; Yang et al., 2010). The suggestive roles of α -syn in synaptic physiology includes synaptic plasticity (Watson et al., 2009), expression and intracellular distribution of synaptic and cytoskeletal proteins like SNARE (Chandra et al., 2005), recycling of synaptic vesicles (Nemani et al., 2010) as well as synthesis and release of neurotransmitter especially dopamine (Abeliovich et al., 2000; Wu et al., 2009; Lou et al., 2010; Gaugler et al., 2012).

α -syn could be detected in biological fluids such as cerebrospinal fluid (CSF) and blood plasma under both normal and PD conditions (El-Agnaf et al., 2003; Tokuda et al., 2006). Besides, it was also found to be secreted by cultured cells overexpressing α -syn into culture medium (Sung et al., 2005). Secretability of α -syn could be implicated in progressive nature of neurodegenerative disorders like PD in which the disease pathology start stage-by-stage from olfactory bulb to brain stem and finally in neocortex as described in Section

2.2.1. Besides, host-to-graft transmission of α -syn-associated pathology has been suggested by several *in vivo* studies in which the α -syn-rich inclusion bodies were observed in grafted neurons many years after transplantation in PD patients (Li et al., 2008; Kordower et al., 2008). These findings suggest propagation behavior of α -syn. However, the exact mechanism of α -syn secretion and propagation remains poorly understood and whether α -syn phosphorylation plays a role in these behaviors needs further elucidation.

2.2.4 Phosphorylation of α -syn

Several post-translational modifications like phosphorylation, ubiquitinylation, truncation, nitration and oxidative modification have been observed in α -syn (Stefanis 2012). Among these, the functional consequences of α -syn phosphorylation especially in the pathogenesis of PD are the most completely studied. α -syn is subjected to phosphorylations at several amino acid residues, including serine and tyrosine. Common phosphorylation sites of α -syn include S87, S129, Y125, Y133 and Y136 (Braithwaite et al., 2012). Among these phosphorylation sites, S87 and S129 are the most intensively studied since most of the α -syn found in Lewy body are phosphorylated at these two sites, with α -syn phosphorylated at S129 being more dominant than that of S87 (Okochi et al., 2000; Fujiwara et al., 2002; Anderson et al., 2006).

Kinases and phosphatases are involved in the regulation of α -syn phosphorylation. A group of kinases such as polo-like kinases (PLK) (Inglis et al., 2009), casein kinases 1 and 2 (CK1 and CK2) (Okochi et al., 2000), G-

protein-coupled receptor kinases (GRK) (Sakamoto et al., 2009), leucine-rich repeat kinase 2 (LRRK2) (Qing et al., 2009) and tyrosine kinase (Ellis et al., 2001) have been implicated in α -syn phosphorylation. These kinases show redundancy in terms of their target sites. For example, several kinases like GRK, CK and PLK could phosphorylate α -syn at S129. This may complicate the kinase-based therapeutic approach in which inhibition of one kinase may cause the upregulation of another kinases to compensate the former one (Braithwaite et al., 2012).

α -syn phosphorylation is reduced by the action of phosphatase such as phosphoprotein phosphatase 2A (PP2A). *In vivo* study using α -syn-transgenic mice has shown that by suppressing the demethylation of B α -containing PP2A via eicosanoyl-5-hydrotrptamide which would then activate the enzyme, there were reduced number of S129-phosphorylated α -syn and α -syn aggregates in the brain (Lee et al., 2011).

It is important to note that α -syn phosphorylation could be a physiological process as suggested by studies showing that S129-phosphorylated α -syn could also be detected in plasma (El-Agnaf et al., 2003), CSF (Tokuda et al., 2006) and brains (Muntane et al., 2012) of normal subjects. Besides, phosphorylated α -syn was also found to be increased with normal aging process which could be attributed to the increased expression of PLK in neurons of older primate (McCormack et al., 2012). Since aging is one of the important risk factor of sporadic PD (Allam et al., 2005), increased level of phosphorylated α -syn may be implicated in PD pathogenesis.

2.2.4.1 Effect of Phosphorylation on α -syn Aggregation and Toxicity

Presence of Lewy bodies in PD patients somehow relates protein aggregation to the etiology of PD. This was supported by evidence that α -syn as the major component of Lewy bodies could self-aggregate and fibrillize *in vitro* to form aggregates (Hashimoto et al., 1998). Phosphorylation has been shown by many *in vitro* and *in vivo* studies to play a role in aggregation and toxicity of α -syn.

Studies focus on S129 phosphorylation yielded inconsistent results. Fujiwara et al. (2002) showed that phosphorylation at S129 residue in α -syn could promote fibril formation *in vitro*. This is supported by findings obtained in SH-SY5Y cell (Smith et al., 2005) and rat model (Gorbatyuk et al., 2007) using phosphorylation mutant constructs. However, the same results were not reproduced in other studies using fly model (Chen and Feany 2005) and rat model (McFarland et al., 2009). Study in fly model even revealed that both phosphorylation mutant and authentic phosphorylation of α -syn at S129 could enhance toxicity via decreasing the aggregates in neuron (Chen and Feany 2005) of which this has challenged the concept of aggregation-mediated neurotoxicity and degeneration. Apart from questionable utilization of phosphorylation mutant constructs in giving the effects of S129 authentic phosphorylation (Paleologou et al., 2008), species difference and interplay between phosphorylation sites may contribute to the results inconsistency. Nonetheless, recent finding derived from PP2A targeting showed that after dephosphorylation of S129 residues due to the effect of PP2A, α -syn aggregates significantly reduced, while both neuronal activity and motor

performance in mouse improved indicative of neuroprotection. This again highlights the significant relevance of S129 phosphorylation to α -syn aggregation (Lee et al., 2011).

Studies on S87 phosphorylation using phosphomimic mutant found that it could suppress α -syn aggregation and prevent neuronal loss as well as motor impairment in rat (Paleologou et al., 2010; Oueslati et al., 2012). Different from S129 phosphomimic mutant, S87 was demonstrated to be able to reproduce the effects of authentic phosphorylation (Paleologou et al., 2008), further enhancing the reliability of the result. It is also important to note that S87 is the only one among phosphorylation sites that lies within the central hydrophobic region or NAC of α -syn which is highly associated to the aggregation properties of the protein (Figure 2.1). This further highlights the implication of S87 phosphorylation in α -syn aggregation.

Apart from disputable α -syn aggregation, α -syn is found to be involved in the regulation of tyrosine hydroxylase (TH) which serves as the rate-limiting enzyme of dopamine synthesis (Daubner et al., 2011). Dopamine could be one of the sources of oxidative stress to cell, which may lead to dopaminergic neuronal degeneration as seen in PD patients (Bisaglia et al., 2010). Overexpression of α -syn could reduce the activity of TH (Perez et al., 2002). However, studies found that phosphorylated α -syn at S129 could reverse the effects by up-regulating the TH activity via increasing TH phosphorylation (Wu et al., 2009; Lou et al., 2010). Hence, α -syn phosphorylation may induce cellular toxicity via dopamine and TH regulation.

2.3 γ -syn

2.3.1 Structure, Properties and Functions of γ -syn

Human γ -syn consists of 127 amino acid residues (Lavedan 1998). Similar to other synuclein, it is believed to be not possessing any defined structure (Biere et al., 2000). Within the synuclein family in which all the three members share high sequence homology, γ -syn is the least conserved protein member, especially at the C-terminal region at which it completely diverges from and is relatively shorter than other members (Buchman et al., 1998). This may account for the different subcellular localization of γ -syn from α -syn in which the former prefers cytosol while the latter prefers nucleus (Specht et al., 2005).

γ -syn, as with other synuclein could aggregate (Uversky and Fink 2002). However, it has lower aggregation potential as compared to α -syn. This may account for the absence of γ -syn in Lewy body which contains high level of α -syn although they are highly similar (Biere et al., 2000). Besides, similar to α -syn, γ -syn was found to be secreted out of the cells as demonstrated in neuronal cell culture (Surgucheva et al., 2012). The same study also revealed that γ -syn could induce α -syn aggregation, but not β -syn.

The function of γ -syn is poorly understood. It is thought to play a role in the development of nervous system due to its developmentally-regulated expression. γ -syn mRNA and protein is abundant in adult brain structures, but absent in embryonic neonatal and forebrain structure. Besides, the time of γ -syn expression is on embryonic days 10 and 11 of which it match with the time when trigeminal ganglions are growing to their targets (Buchman et al.,

1998). Apart from this, it may play a role in the regulation of microtubule (Zhang et al., 2011), neurofilament network (Buchman et al., 1998) and cellular signalling (Surgucheva et al., 2008).

2.3.2 Association of γ -syn with Neurodegenerative Diseases

As compared to α -syn, γ -syn is less often be associated with PD since it is not detected in Lewy bodies. However, Galvin et al. (1998) have detected axonal β - and γ -syn-containing lesions in the hippocampal dentate molecular layer of PD brain but not in normal control brain. This study suggests that interplay between synuclein proteins may be responsible in the complicated pathogenesis of PD. This is further supported by observation that γ -syn could promote the α -syn aggregation *in vitro* and in cell cultures of which this effect could be enhanced when γ -syn is oxidized (Surgucheva et al., 2012).

γ -syn was also found to be associated with glaucoma, a disease which is characterized by deterioration of optic nerve associated with selective apoptotic death of retinal ganglion cell (RGC) which would eventually cause blindness on the patients (Surgucheva et al., 2008). In the optic nerve bundles of glaucoma patients and normal individual, γ -syn was detected. However, in the glaucoma rat model, both γ -syn mRNA and protein in the optic nerve appeared to reduce in the course of glaucomatous alteration in which this may suggest that change of expression profile for γ -syn occurs in glaucoma condition (Surgucheva et al., 2002). γ -syn knockdown study in RGC-5 cell revealed that γ -syn silencing may reduce the phosphorylation of Bad protein,

which belongs to Bcl-2 family that play roles in apoptotic pathway. This would initiate apoptotic death cascade, resulting in retinal ganglion cell death as occurred in glaucoma (Surgucheva et al., 2008). The functions of γ -syn in nervous system is still a gray area. However, its association with neurodegenerative diseases could not be neglected and further elucidations are required to gain new insights for better understanding of the underlining mechanisms.

2.3.3 Association of γ -syn with Cancers

The process of cancer development is complex in which multiple stages are involved. During the process of transformation into tumor cells, many genetic mutations accumulate within the normal cells. This eventually makes the transformed cells to obtain phenotypes of autonomous growth factor signaling, irresponsiveness to growth inhibitory signal, resistance to apoptosis, unlimited replicative potential, angiogenesis and ability to invade and metastasize (Hanahan and Weinberg 2000). γ -syn is found to be overexpressed in advanced stages of breast cancer carcinoma while remained undetectable in normal or benign breast tissues (Ji et al., 1997). Besides, stage-specific expression of γ -syn also occurs in other cancer types including ovarian, cervical, prostate, esophagus, colon, lungs, bladder and liver (Liu et al., 2005). These findings suggested that γ -syn expression could be linked to the process of tumorigenesis.

Since sequence studies done on the DNA obtained from ovarian tumors overexpressing γ -syn found no evidence of mutation and amplification of *SNCG* gene, transcriptional deregulation could be responsible for the aberrant expression (Bruening et al., 2000). Methylation status of the *SNCG* gene could be involved in the regulation of the γ -syn expression since hypomethylated *SNCG* gene has been discovered in many cancer types overexpressing γ -syn (Liu et al., 2005; Zhao et al., 2006).

Gene silencing using siRNA strategy revealed that γ -syn could reduce cellular apoptotic death induced by anti-microtubule-based chemotherapeutic agents like paclitaxel but not DNA repair reagents (Zhou et al., 2006). This is further confirmed by study made by Zhang et al. (2011) which suggested that γ -syn overexpression may increase resistance to chemotherapeutic agent through reducing microtubule rigidity. Besides, another siRNA gene silencing study revealed that γ -syn knockdown could inhibit the cell proliferation and migration induced by insulin-like growth factor I (Li et al., 2010). γ -syn also involves in upregulation of matrix metalloproteinases (MMP), which would assist in invasion and metastasis of cancer cells by degradation of extracellular matrix (Surgucheva et al., 2003).

2.4 *In Vitro* Site-Directed Mutagenesis

In vitro site-directed mutagenesis is an invaluable technique for studying structure-function relationship of protein. Using this technique, mutations could be created precisely at specific residue to change the codon which will

produce desired amino acid substitution in the protein of interest. By comparing the mutant protein to the wild type protein, the structural and functional roles of the amino acid could be investigated (Ling and Robinson 1997; Zawaira et al, 2012). There are many approaches for this technique, of which some require single-stranded DNA (ssDNA) as the template, which would be labor intensive due to the need to subclone the mutated sequence into M13-based bacteriophage vector and for ssDNA rescue (Primrose and Twyman 2006). Circular mutagenesis is one of the dsDNA-based approaches and it applies whole-plasmid amplification. It could be used to address for these limitations.

QuickChange™ Site-Directed Mutagenesis Protocol (QCM) developed by Stratagene is probably the most favored method which has applied circular mutagenesis (Liu and Naismith 2008; Zawaira et al., 2012). This method is short and thus could speed up the mutagenesis process without incurring much reagent costs (Zawaira et al., 2012). It works by incorporating a pair of complementary mutagenic primers that span the targeted mutagenesis site into PCR thermal cycling process (Figure 2.4). Along the PCR thermal cycling, the primers extend in opposite direction, generating two complementary linear mutant DNA strands that are able to form double-stranded circle with staggered nicks. The PCR products are then treated with *DpnI* endonuclease (target sequence: 5'-Gm6ATC-3') which is specific for methylated and hemi-methylated DNA. This would remove the highly-methylated parental DNA template while select for unmethylated mutant strands. The double-stranded

circles with staggered nicks are then transformed into competent cells for nick repairing and propagation of plasmids with desired mutation.

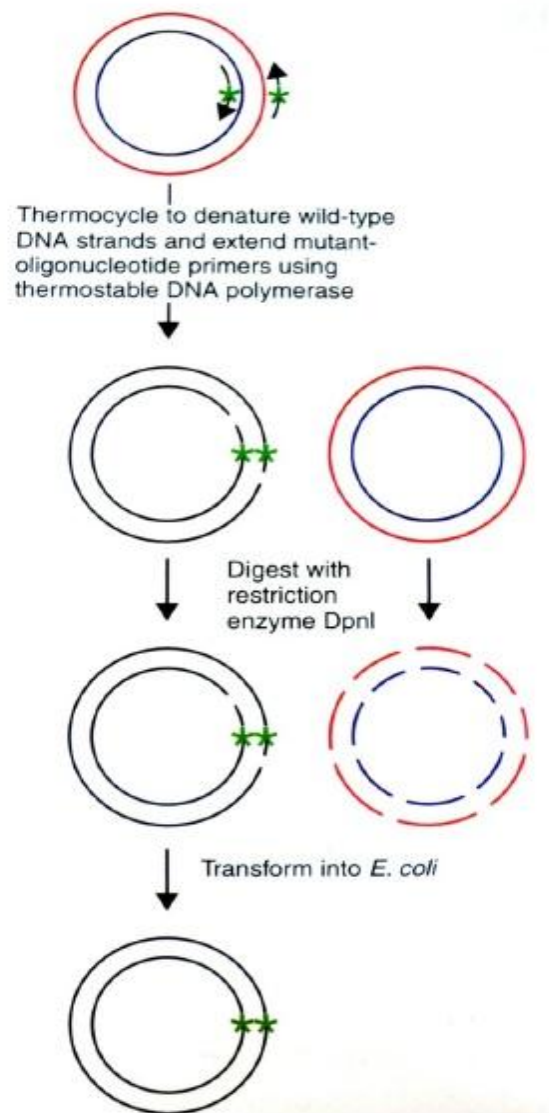


Figure 2.4: Schematic diagram of Stratagene QuickChange™ Site-Directed Mutagenesis Protocol (QCM). Adapted from Reece (2004).

It is important to use low PCR cycle number (usually 16 cycles) in QCM method. If the hybrid (nicked mutant and circular parent) plasmid strands are involved in primer-binding events, the mutant strand would lose the circularity. The chance for primers binding to the hybrids increases with the PCR cycle number and hence, beyond certain threshold (usually 16 cycles), the yield of mutant strands would be reduced with increasing cycle number (Zawaira et al., 2012). Besides, it is also important to use DNA polymerase with high fidelity and without strand-displacement activity such as *Pfu* DNA polymerase (Sambrook and Russell 2001) in this method. DNA polymerase with strand-displacement activity is able to displace the encountered DNA at downstream during primer extension process. Once reaching 5' end of the primer after amplifying the whole plasmid, they would displace the newly synthesized mutant strand and continue the extension reaction which would affect the mutagenesis process (New England Biolabs n.d.).

QCM method has two major disadvantages. First, it favors the formation of primer dimer because both the forward and reverse mutagenic primers used are completely complementary to each other (Liu and Naismith 2008) which may contribute to low or no yield of final amplification products. Second, it has low amplification efficiency which could be due to low PCR cycle number as elaborated before and the fact that nicked amplification products could not be used as template for subsequent amplification (Liu and Naismith 2008). In addressing to the low amplification efficiency due to strong primer dimer formation, variant of QCM method like Single-Primer Reactions In Parallel (SPRINP) could be performed (Edelheit et al., 2009). In this method, two

separate amplification reactions with each containing single primer species (either forward or reverse) are performed, thus reducing primer dimer problem as encountered in QCM method (Edelheit et al., 2009).

2.5 RNA Interference (RNAi)

RNAi was first discovered by Andrew Fire and Craig Mello in nematode, *Caenorhabditis elegans* to be involved in the sequence-specific suppression of gene expression. They demonstrated that double stranded RNA (dsRNA) is much more potent in gene silencing compared to single stranded antisense reagents which had long been used in laboratory (Fire et al., 1998). RNAi could also occur in human, plants and worm of which this suggested that the cells contain a set of proteins that recognize and process dsRNA (Gonzalez-Alegre and Paulson 2007). Besides, mammalian genomes encodes for hundreds of endogenous dsRNA molecules, known as microRNAs (miRNAs), which also serve to regulate expression of protein-coding genes in mammal (Bentwich et al., 2005).

RNAi pathway (Figure 2.5) consists of two dedicated ribonucleases (RNase III) enzymes, known as Drosha and Dicer (Carmell and Hannon 2004). Drosha serves to mediate nuclear processing of endogenous primary miRNAs (pri-miRNAs) transcribed from miRNAs genes into ~70 nucleotides stem-loop hairpin structure known as precursor miRNAs (pre-miRNAs) which are then translocated to the cytoplasm via exportin-5-mediated mechanism (Bartel 2004). Dicer serves to process the pre-miRNAs into smaller intermediates

with two strands, known as small interfering RNAs (siRNAs) (Cullen 2004). siRNA contains a guide (or antisense) and a passenger strand. The guide strand will then be incorporated into the RNA-induced silencing complex (RISC) which contains the endonuclease Argonaute 2 (AGO2). AGO2 serves in cleavage of bound target mRNA that is completely complementary to the guide strand (Meister et al., 2004). The cleaved mRNA is destroyed rapidly, making the RISC-guide strand complex available for cleavage of other target mRNA, thus resulting in suppression of targeted gene (Gonzalez-Alegre and Paulson 2007).

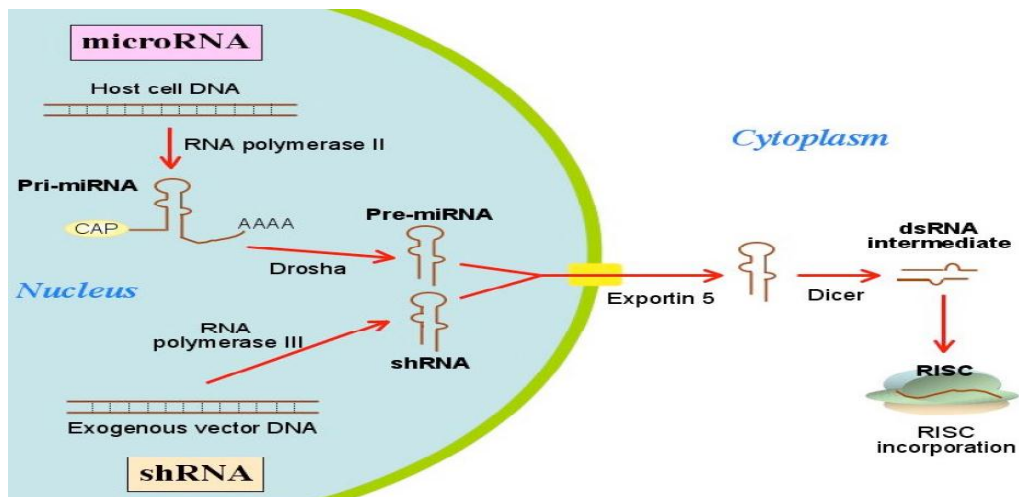


Figure 2.5: Schematic diagram of RNAi pathway. Endogenous miRNA genes are transcribed by RNA polymerase II, whereas exogenous vector DNA like plasmid templates are transcribed by RNA polymerase III into shRNA which are functionally and structurally equivalent to pre-miRNAs (Nikolova and Toncheva 2008).

When dsRNAs more than 30 bp in length were used to study gene function in most of the mammalian cells, it was observed that the proteins translation

within the cells was inhibited, which could be attributed to activation of interferon (IFN) system (Zhou et al., 2010). These cellular responses could lead to cell death via apoptosis in mammalian cells, impeding the use of RNAi in mammalian cells (Paddison et al., 2002). In order to use RNAi without inducing the IFN activation in mammalian cells, 21-22 bp-long synthetic siRNAs that bypass Dicer enzymatic step could be used (Zhou et al., 2010). Plasmid vectors expressing shRNA could also be used (Zhou et al., 2010) (Figure 2.3) and they are better than synthetic siRNAs in terms of silencing longevity and cost (McIntyre and Fanning 2006).

CHAPTER 3

MATERIALS AND METHODS

3.1 List of Materials and Apparatus

The list of apparatus and equipment used for this study and their respective manufacturers is shown in Table 3.1. The list of material used for this study and their respective manufacturers is shown in Table 3.2. The list of solutions used for this study and their respective formulation is shown in Table 3.3.

Table 3.1: List of apparatus and equipment used for this study and their respective manufacturers.

Apparatus/Machine/Equipment	<i>Manufacturer, Country</i>
ABJ Electronic balance	<i>Kern, Germany</i>
Autoclave sterilizer	<i>Hirayama, Japan</i>
Centrifuge	<i>Dynamica, Australia</i>
Desktop computer	<i>Dell, Malaysia</i>
Electrophoresis system	<i>Major Science, USA</i>
Ice maker	<i>Hoshizaki, UK</i>
Imaging system	<i>Syngene Bioscience, India</i>
Incubator	<i>Memmert, Germany</i>
Laminar hood flow	<i>ESCO, Singapore</i>
Microcentrifuge	<i>Sigma, UK</i>

Table 3.1 (continued):

Apparatus/Machine/Equipment	Manufacturer, Country
Micropipette	<i>Gilson (Pipetman) (1-10 µL) (10-100 µL) (100-1000 µL), USA</i>
Microwave	<i>Sharp, Australia</i>
Nano-spectrophotometer	<i>Implen, Germany</i>
PCR-thermocycler	<i>Eppendorf, Germany</i>
Refrigerator	<i>Thermo Scientific, USA</i>
Shaking incubator	<i>Daihan Lab Tech Co. Ltd, Korea</i>
Spectrophotometer	<i>Biorad, USA</i>
Water bath	<i>Memmert, Germany</i>
Water system	<i>Purelab (Option Q), Australia</i>

Table 3.2: List of material used for this study and their respective manufacturers.

Material	Manufacturer, Country
1 kb DNA ladder	<i>Vivantis, Malaysia</i>
50 bp DNA ladder	<i>Philekorea Technology, Korea</i>
95% ethanol	<i>Copens Scientific, Malaysia</i>
Agarose powder	<i>Vivantis, Malaysia</i>
Ampicillin sodium	<i>USB, Italy</i>
Annealing buffer	<i>New England Biolabs (10 × NEBuffer 2), UK</i>
Bovine Serum Albumin	<i>EURx (100 × BSA), Poland</i>

Table 3.2 (continued):

Material	Manufacturer, Country
Dimethyl sulphoxide (DMSO)	<i>R&M Marketing, UK</i>
DNA ligase	<i>New England Biolabs (T4 DNA ligase), UK</i>
DNA ligase buffer	<i>New England Biolabs (10 × NEB T4 DNA ligase buffer with 10mM ATP), UK</i>
Gel DNA recovery kit	<i>Vivantis, Malaysia</i>
Glycerol (99.5%)	<i>QReC, Malaysia</i>
Ethylenediaminetetraacetic acid (EDTA)	<i>System, Malaysia</i>
Ethidium bromide	<i>Bio Basic Inc., Canada</i>
Isopropanol	<i>MERCK, Germany</i>
LB broth powder	<i>Laboratorios Conda Pronadisa (Miller's LB broth), Spain</i>
LB agar powder	<i>Laboratorios Conda Pronadisa (Miller's LB agar), Spain</i>
Magnesium chloride hexahydrate	<i>QReC, Malaysia</i>
Mutagenic Primers (PCR Grade)	<i>Ist Base, Malaysia</i>
Oligonucleotides (Trityl-On Oligonucleotide Purification)	<i>Ist Base, Malaysia</i>
<i>Pfu</i> DNA polymerase	<i>Philekorea Technology (X-Pfu DNA Polymerase), Korea</i>
PCR buffer	<i>Philekorea Technology (10 × PCR buffer, 50mM MgCl₂, 10mM dNTP Mix), Korea</i>
Plasmid extraction kit: Minipreparation	<i>Fermentas, USA</i>
Midipreparation	<i>Qiagen, Germany</i>

Table 3.2 (continued):

Material	Manufacturer, Country
Restriction enzyme : <i>AgeI</i>	<i>Fermentas</i> , USA
<i>DpnI</i>	<i>Fermentas</i> , USA
<i>EcoRI</i>	<i>Fermentas</i> , USA
<i>NcoI</i>	<i>New England Biolabs</i> , UK
<i>XhoI</i>	<i>EURx</i> , Poland
Restriction enzyme buffer	<i>Fermentas</i> (10 × Buffer O, 10 × <i>EcoRI</i> Buffer), <i>EURx</i> (10 × Buffer Medium), USA
Tris	<i>MP Biomedicals</i> , France

Table 3.3: List of solutions used for this study and their respective formulation.

Solution	Formulation
CaCl ₂ solution	0.1 M CaCl ₂
LB ampicillin agar	Tryptone 1%, Yeast extract 0.5% , NaCl 1%, agar 1.5%, pH 7 at 25 °C, sterilization by autoclaving, addition of ampicillin to a final concentration 50 µg/ mL when agar is cool.
LB ampicillin broth	Tryptone 1%, Yeast extract 0.5%, NaCl 1%, pH7 at 25 °C, sterilization by autoclaving, addition of ampicillin to a final concentration of 50 µg/mL.
Loading dye	30% (v/v) glycerol, 0.25% (w/v) bromophenol blue, 0.25% (w/v) xylene cyanol

Table 3.3 (continued):

Solution	Formulation
TAE buffer	20 mM Tris, pH 8.0, 2 mM Glacial acetic acid, 1 mM EDTA
TE buffer	10 mM Tris HCl, pH 7.92, 1 mM EDTA

3.2 Molecular Biology of α -syn Phosphorylation Mutant Constructs

3.2.1 Mammalian Expression Vector, pcDNATM3.1D/V5-His-TOPO with Full-length Wild Type Human α -syn

Plasmid pcDNATM3.1D/V5-His-TOPO cloned with full-length wild type human α -syn (GenBank ID: BC108275.1) cDNA (Clone ID: 6147966) (pcDNATM3.1D/V5-His-TOPO WT α -syn) which had been previously established in our lab (Choong 2011) was used as the template for site-directed mutagenesis. Important elements of the plasmid vector are shown in Figure 3.1. TOPO cloning site serves as the site in the plasmid vector for directional cloning of full-length wild type human α -syn as an insert. T7 priming site enables the *in vitro* transcription and sequencing through the insert. Human cytomegalovirus (CMV) promoter enables high-level expression of recombinant protein. Ampicillin resistance gene serves as the selection marker for the plasmid in *E. coli*. Neomycin resistance gene serves as the selection marker for the plasmid in mammalian cells. High-copy number replication of the plasmid is permitted due to presence of pUC origin. Several single-cutter restriction sites including *Xho*I restriction site in the plasmid enable revealing of total plasmid length.

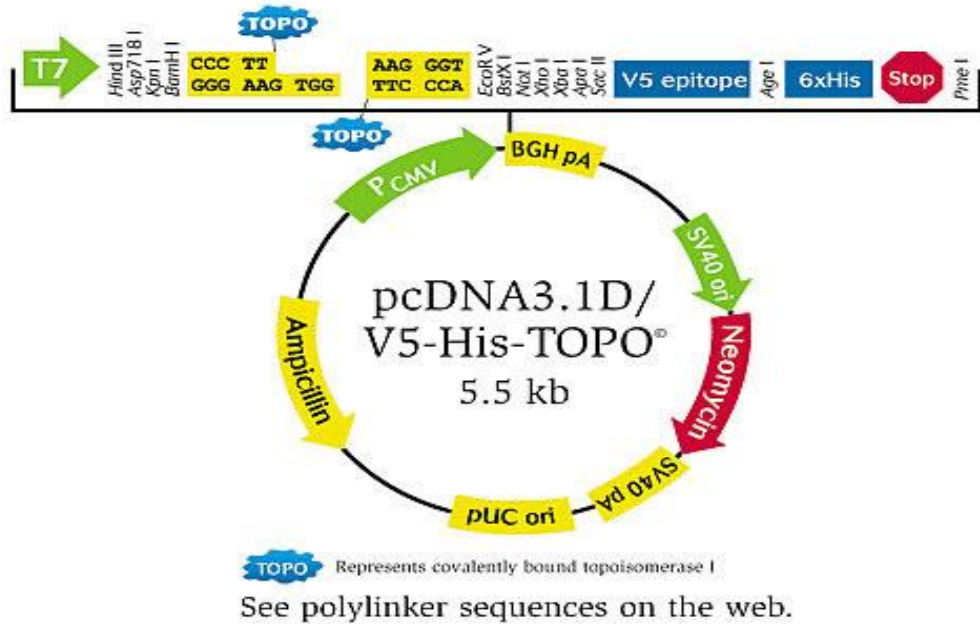


Figure 3.1: Map of pcDNATM3.1D/V5-His-TOPO vector. Adapted from Invitrogen (2013).

3.2.2 Primer Design for Generation of α -syn Phosphorylation Mutant Constructs

Several considerations as recommended in QuickChangeTM Site-Directed Mutagenesis Protocol kit's instruction manual were taken when designing mutagenic primers. First, primers must contain desired mutation and anneal to the same sequence for both strands. Second, primers must have 25-45 bases in length, with melting temperature (T_m) greater or equal to 78 °C. Third, they must have desired mutation in the middle of primer, flanked by 10-15 correct bases on both sides. Forth, they must have minimum GC content of 40% and should terminate in one or more C or G bases.

Primer design for generation of α -syn mutant constructs including S87A, S87D, S129A and S129D was done using PrimerX Automated Mutagenic Primer Design Program available online at <http://www.bioinformatics.org/primerx/index.htm>. The forward and reverse primers for each mutant construct are shown in Table 3.4.

Table 3.4: Forward (F) and reverse (R) primers used for generation of α -syn phosphorylation mutant constructs and their respective sequences.

Primers	Primers Sequence (5' to 3')
S87A (F)	GTGGAGGGAGCAGGGG <u>GCG</u> ATTGCAGCAGCCAC
(R)	GTGGCTGCTGCAAT <u>CGCC</u> CTGCTCCCTCCAC
S87D (F)	GGAGGGAGCAGGGG <u>GAC</u> ATTGCAGCAGCC
(R)	GGCTGCTGCAATG <u>TCC</u> CTGCTCCCTCC
S129A (F)	GAGGCTTATGAAATGCCT <u>GCGG</u> GAGGAAGGGTATCAAGAC
(R)	GTCTTGATACCCTTCCT <u>CCGC</u> AGGCATTCATAAGCCTC
S129D (F)	GGCTTATGAAATGCCT <u>GAT</u> GAGGAAGGGTATCAAG
(R)	CTTGATACCCTTCCTC <u>ATC</u> AGGCATTCATAAGCC

*Underlined nucleotides represent mutations incorporated in the primer.

3.3 Preparation of Chemical Competent Cells

E. coli DH5 α or JM109 was inoculated from glycerol stock into a new LB agar plate using streak plate technique to isolate single colony. The plate was incubated overnight at 37 °C. On the next day, single colony was inoculated into 50 mL of LB broth in a 250 mL conical flask. The conical flask was

incubated overnight at 37 °C with shaking at 200 rpm. On the following day, 1 mL of the overnight culture was inoculated into 25 mL of LB broth in 100 mL conical flask and then incubated for 2-3 hours at 37 °C with shaking at 200 rpm. Optical density at 600 nm (OD₆₀₀) of the culture was monitored every 45 minutes. OD₆₀₀ of LB broth was set as blank. OD₆₀₀ (1 OD₆₀₀ equals 1×10^9 cells/mL) of the culture for competent cell preparation should lie between 0.6-1.0 with the best reading being 0.6. Then, the culture was immediately transferred to a pre-chilled centrifuge tube and stored on ice. The tube was then centrifuged at 4100 rpm for 10 minutes at 4 °C. All supernatant was discarded before the pellet was resuspended by swirling with 10 mL of pre-chilled MgCl₂-CaCl₂ solution. Then, the tube was centrifuged at 4100 rpm for 10 minutes at 4 °C. All supernatant was discarded before the pellet was resuspended by swirling with 2 mL of pre-chilled CaCl₂ solution. The cells were then either being kept on ice for 2 hours before stored in 16% glycerol stock for long term storage or transformed directly with plasmid. To achieve better transformation efficiency, the cells were stored at 4 °C for 12-24 hours before used for subsequent transformation (Sambrook and Russell 2001).

3.4 Cell Competency Test

3.4.1 Heat Shock Transformation

Competent cells with the volume of 99 µL were added into pre-chilled 1.5 mL microcentrifuge tube. One microliters of plasmid pcDNATM3.1D/V5-His-TOPO WT α -syn with the concentration of 24 ng/µL was added into the competent cells. The transformation reaction was mixed by gently tapping the

tube before incubated on ice for 30 minutes. After cold incubation, the transformation reaction was heat-pulsed for 45 seconds at 42 °C and then placed back to ice and incubated for another 10 minutes. After that, 900 µL of pre-warmed LB broth was added to the transformation reaction and the reaction was then incubated at 37 °C for 1 hour with shaking at 200 rpm.

3.4.2 Serial Dilution

After incubation at 37 °C for 1 hour, 100 µL of transformation reaction was transferred to 900 µL of LB broth in another microcentrifuge tube. After mixing thoroughly, 100 µL of the diluted cells was spread to LB-ampicillin agar plate. Dilution factor of 100 was obtained after this serial dilution. The plate was then incubated at 37 °C for overnight to allow growth of transformed colonies. The colonies obtained were counted. The cell competency was calculated using the formula below:

$$\text{Cell competency} = [\text{number of colonies} / \text{concentration of plasmid (ng)}] \times 100 \\ \times 1000$$

3.5 Propagation of Plasmid Template in *dam*⁺ *dcm*⁺ *E.coli*

3.5.1 Transformation and Plasmid Extraction (Midipreparation)

A well-isolated transformed colony on transformation plate obtained from heat shock transformation protocol elaborated in Section 3.4 was inoculated into 5 mL of LB ampicillin broth in 50 mL centrifuge tube as starter culture. The

starter culture was incubated for 8 hours at 37 °C with shaking at 200 rpm. After that, 50 µL of starter culture was inoculated into 50 mL of LB ampicillin broth in 250 mL conical flask and incubated overnight at 37 °C with shaking at 200 rpm. Bacterial cells were harvested by centrifugation at 6000 × g for 15 minutes at 4 °C. The supernatant was discarded. The plasmid DNA was purified using Qiagen Plasmid Midi Kit according to the protocol illustrated in the manufacturer's handbook. The plasmid DNA was eluted in 50 µL of TE buffer.

Purified plasmid was then analysed using nanospectrophotometer with absorbance reading at 260 nm and 280 nm. Concentration of plasmid DNA was determined by absorbance reading at 260 nm. Purity of the plasmid DNA was deduced from the ratio of A₂₆₀:A₂₈₀ (DNA: protein) where ratios ranging from 1.8 to 2.0 indicate high purity.

3.5.2 Linearization of Plasmid

A 25 µL reaction mix consisting of 1.2 µg of plasmid DNA, 0.5 µL of BSA (100 ×), 2.5 µL of 10 × buffer medium, 0.3 µL of *Xho*I (15 U/µL) and autoclaved distilled water topped up to 25 µL was incubated at 37 °C for 15 hours. One microliters of the reaction volume was mixed with 1 µL of 6 × loading dye before being electrophoresed on a 1% agarose gel at 90 V for 40 minutes to verify the digestion products.

3.6 Mutant Strand Synthesis

3.6.1 Stratagene QuickChange™ Site-Directed Mutagenesis Protocol

PCR was carried out according to proportion of reaction components (Table 3.5) and thermal cycling conditions recommended in instruction manual with slight modification. DMSO was added into the PCR reaction in order to inhibit the secondary structures of DNA template and primer, increasing chance of primer-template annealing. Thermal cycling condition used was 3 minutes of initial denaturation at 95 °C, followed by 16 cycles of 94 °C for 2 minutes, 55 °C for 1 minute and 70 °C for 4 minutes. After PCR thermal cycling, 1 µL of *DpnI* (10 U/µL) was added into the PCR reactions and the whole reaction was incubated at 37 °C for 1 hour to digest the parental DNA template. Then, 4 µL of post-*DpnI*-PCR product was transformed into 50 µL of competent *E. coli* DH5α using heat shock method as described in Section 3.4.1. After incubation of transformation reactions at 37 °C for 1 hour with shaking at 200 rpm, the cells were pelleted by centrifugation at 10,000 rpm and 750 µL of LB broth was discarded. The remaining 250 µL of LB broth was used to resuspend the pellet before being spread on LB ampicillin agar plates. The plates were then incubated at 37 °C overnight to allow the growth of transformed colonies.

Table 3.5: Composition of PCR reaction (QCM) used for α -syn phosphorylation mutant constructs (S87A, S87D, S129A and S129D).

Reagent	Volume (1 \times Reaction)	[Final]*
10 \times PCR Buffer	2 μ L	1 \times
50mM MgCl ₂	0.4 μ L	1 mM
10mM dNTP mix	0.4 μ L	0.2 mM
125 μ g/mL Forward Primer	0.4 μ L	2.5 ng/ μ L
125 μ g/mL Reverse Primer	0.4 μ L	2.5 ng/ μ L
24 μ g/mL dsDNA template	0.8 μ L	1 ng/ μ L
DMSO	0.6 μ L	NA*
ddH ₂ O	14.7 μ L	NA*
<i>Pfu</i> DNA polymerase (5 U/ μ L)	0.3 μ L	1.625 U
Total Reaction	20 μ L	NA*

* NA refers to non-applicable, [Final] refers to final concentration.

3.6.2 Single Primer Reaction in Parallel

In order to reduce the primer dimer problem encountered when performing QCM as described in Section 3.6.1, two separate PCR reactions containing either forward primer or reverse primer were carried out using the protocol described by Edelheit et al. (2009) with slight modification (schematic diagram shown in Appendix A). The PCR reaction components used are shown in Table 3.6. Thermal cycling conditions used were 2 minutes of initial denaturation at 94 $^{\circ}$ C, followed by 30 cycles of 94 $^{\circ}$ C for 2 minutes, 55 $^{\circ}$ C for 1 minute and 70 $^{\circ}$ C for 4 minutes. After PCR thermal cycling, two PCR products (Reaction 1 and Reaction 2) were combined and then heated to 95 $^{\circ}$ C for 5 minutes in a thermal cycler to promote denaturation of PCR product from parental plasmid template.

Then, the tube was slowly cooled to 37 °C to promote re-annealing of denatured parental plasmid template and PCR products. The slow cooling condition was 90 °C for 1 minute, followed by 80 °C for 1 minute, 70 °C for 0.5 minute, 60 °C for 0.5 minute, 50 °C for 0.5 minute, 40 °C for 0.5 minute and lastly holding at 37 °C. After that, 2 µL of *DpnI* (10 U/µL) was added into the reaction and incubated overnight at 37 °C. The next day, 4 µL of post-*DpnI*-PCR product was transformed into 50 µL of competent *E. coli* DH5α or JM109 using heat shock method as described in Section 3.4.1. The method used after this was similar to the method described in Section 3.6.1.

Table 3.6: Composition of PCR reaction (SPRINP) used for α-syn phosphorylation mutant constructs (S87A, S87D, S129A and S129D).

Reagents	Reaction 1	Reaction 2
dsDNA template	500 ng	500 ng
Forward primer	40 pmol	-
Reverse primer	-	40 pmol
MgCl₂	1 mM	1 mM
dNTP mix	0.2 mM	0.2 mM
10 × PCR buffer	1 ×	1 ×
<i>Pfu</i> DNA polymerase	1.25 U	1.25 U
Final volume	25 µL	25 µL

3.6.3 Plasmid Extraction (Minipreparation), Linearization and Sequencing

A well-isolated transformed colony on transformation plate obtained from mutagenesis process as elaborated in Section 3.6.1 and 3.6.2 was inoculated into 5 mL of LB ampicillin broth and incubated overnight at 37 °C with shaking at 200 rpm. Bacterial cells were harvested by centrifugation at 8000 rpm for 2 minutes at 24 °C. The supernatant was discarded. The plasmid DNA was purified using GeneJET™ Plasmid Miniprep Kit according to the protocol illustrated in the manufacturer's handbook. The plasmid DNA was eluted in 35 µL of autoclaved distilled water. The purified plasmid was then analysed using nano-spectrophotometer to determine the concentration and purity. After that, the purified plasmids were linearized with *XhoI* and the digestion products were visualized on gel using the method elaborated in Section 3.5.2. This was to confirm that the size of purified plasmid was approximately 6 kb before sending to 1st BASE Laboratories Sdn Bhd, Selangor, Malaysia for sequencing using T7 universal primer as sequencing primer.

3.7 Molecular Biology of γ -syn Gene Silencing Constructs

3.7.1 Lentiviral Plasmid pLKO.1 TRC

pLKO.1 TRC is a replication incompetent lentiviral vector preferred by the RNAi Consortium (TRC) for shRNA construction and expression (Moffat et al., 2006). It was used in this study to generate shRNA construct for knockdown of human γ -syn gene. Important elements of the plasmid are shown in Figure 3.2. Human U6 promoter directs RNA polymerase III-

mediated transcription of shRNA insert. Central Polypurine Tract (cPPT) facilitates nuclear penetration of the vector's preintegration complex in the transduced cells without altering the transduction efficiency. Presence of puromycin resistance (Puro R) gene allows the selection of the plasmid vector in mammalian cells. Ampicillin (Amp R) resistance gene allows the selection of plasmid vector in the bacterial cell. Both 5'-Long Terminal Repeat (LTR) and self-inactivating (sin) 3'-LTR present in the backbone of the plasmid to allow the chromosome integration of lentiviral vector genomic RNA which could be packaged into lentiviral vector virions (Tolmachov et al., 2011).

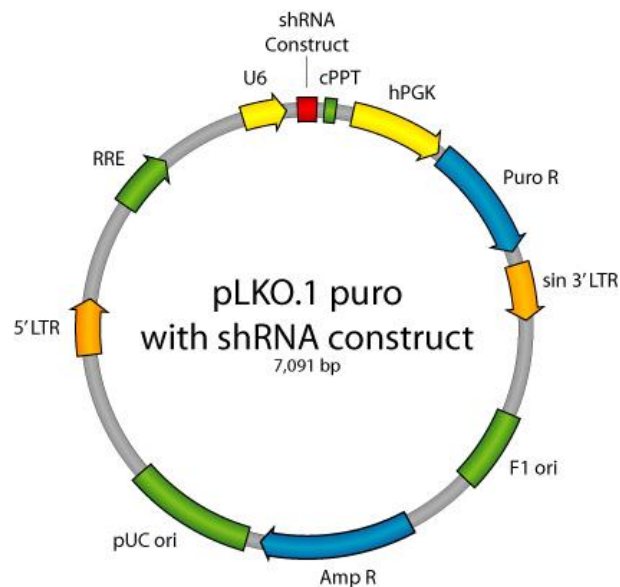


Figure 3.2: Map of lentiviral plasmid pLKO.1 TRC containing a shRNA insert. Original plasmid pLKO.1 TRC has a 1.9 kb stuffer which needs to be released via dual digestion using *AgeI* and *EcoRI* before shRNA oligonucleotide is cloned into the site to replace the stuffer (Moffat et al., 2006).

3.7.2 Design of shRNA Oligonucleotides against Human γ -syn Gene

Suitable 21-mer targets in *SNCG* gene encoding for γ -syn were selected using siRNA Selection Program hosted by Whitehead Institute for Biomedical Research available online at <http://jura.wi.mit.edu/bioc/siRNAext/>. Several considerations were taken for effective gene silencing. First, starting at 25 nucleotides downstream of start codon (ATG), 21-mer sequences that match the pattern AA (N₁₉) where N is any nucleotide, were determined. Second, 21-mer sequences with GC content ranging from 36% to 52% were more preferable. Third, the sense 3' end of the 21-mer sequences with low stability and at least one A or T within position 15-19 were more preferable. Fourth, introns were avoided to be targeted. Fifth, sequences with stretches of four or more nucleotide repeats especially repeated Ts were avoided since polyT is a termination signal for RNA polymerase III. Lastly, the selected sequences were compared to human genome database using NCBI's Blast Program, to make sure that the sequences have at least three nucleotides mismatches to all unrelated gene. Three different sequences to be targeted in *SNCG* gene (Table 3.7) were selected and used in this study since demonstration that different shRNA targeting the same gene can give the same phenotype could alleviate the concern about off-target effects.

Table 3.7: List of 21-mer target sequences in *SNCG* gene for efficient gene silencing.

shRNA construct	21-mer target sequence
γ -syn shRNA 1	5' AAG ACC AAG GAG AAT GTT GTA 3'
γ -syn shRNA 2	5' AAG GAG AAT GTT GTA CAG AGC 3'
γ -syn shRNA 3	5' AAT GTT GTA CAG AGC GTG ACC 3'

As shown in Figure 3.3, in order to synthesize the functional shRNA construct, complementary oligonucleotides were designed to have sense and antisense sequence which is separated by 6-nucleotides spacer, in which the sense sequence is similar to the 21-mer target sequence and the spacer would form a loop once expressed. In order to facilitate cloning of shRNA oligonucleotides into pLKO.1, the complementary oligonucleotides were designed to be flanked by sequences that are compatible with sticky ends of *AgeI* and *EcoRI*. The forward and reverse oligonucleotides for the three shRNA constructs are shown in Table 3.8.

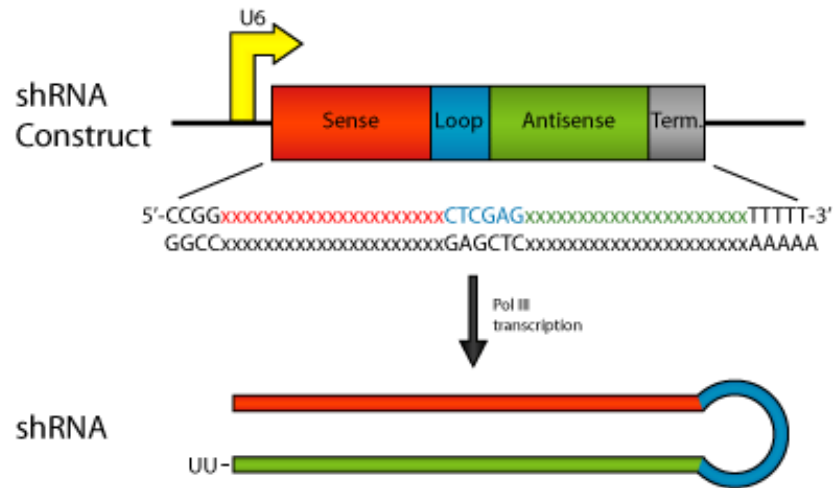


Figure 3.3: Main elements of shRNA complementary oligonucleotides include sense sequence, spacer or loop region and antisense sequence. Polymerase III-mediated transcription of the shRNA is directed by adjacent U6 promoter present in pLKO.1 backbone (Addgene 2006).

Table 3.8: Forward and reverse oligonucleotides for the three γ -syn shRNA constructs.

shRNA construct	Forward oligonucleotide (5'-3')	Reverse oligonucleotide (5'-3')
γ -syn shRNA 1	CCGGAAGACCAAGGAGAATGTTG	AATTCAAAAAAAGACCAAGGAGAAT
	TACTCGAGTACAACATTCTCCTG	GTTGTACTCGAGTACAACATTCTCCT
	GTCTTTTTTTG	TGGTCTT
γ -syn shRNA 2	CCGGAAGGAGAATGTTGTACAGA	AATTCAAAAAAAGGAGAATGTTGTA
	GCCTCGAGGCTCTGTACAACATTC	CAGAGCCTCGAGGCTCTGTACAACA
	TCCTT TTTTTG	TTCTCCTT
γ -syn shRNA 3	CCGGAATGTTGTACAGAGCGTGAC	AATTCAAAAAAATGTTGTACAGAGC
	CCTCGAGGGTCACGCTCTGTACAA	GTGACCCTCGAGGGTCACGCTCTGT
	CATTTTTTTG	ACAACATT

3.7.3 Annealing of shRNA Oligonucleotides

Mixture of 50 μL as shown in Table 3.9 was prepared. The mixture was then incubated in water bath in a 1 L beaker which had been pre-heated to 95 $^{\circ}\text{C}$ - 100 $^{\circ}\text{C}$ using flame of Bunsen burner for 4 minutes. After that, the water bath was allowed to cool to room temperature slowly in a few hours to allow proper annealing of oligonucleotides. Another mixture of 50 μL as shown in Table 3.9 was prepared, however, this mixture was not annealed (no heat-incubation and subsequent slow cooling process). This mixture was used as a negative control to be electrophoresed together with annealed oligonucleotides for γ -syn shRNA 1, 2 and 3 in order to test for the efficiency of oligonucleotide annealing.

Table 3.9: Preparation of mixture for annealing of shRNA oligonucleotides.

Component	Volume
100 μM Forward oligonucleotide	1 μL
100 μM Reverse oligonucleotide	1 μL
10 \times NEBuffer 2	5 μL
Autoclaved ddH ₂ O	43 μL

3.7.4 Dual Digestion of Lentiviral Plasmid pLKO.1 TRC

To release 1.9 kb stuffer, simultaneous dual digestion of pLKO.1 was carried out and the reaction mixture is shown in Table 3.10. The reaction mixture was

incubated at 37 °C for 15 hours. Then, the dual digested DNA was electrophoresed on 0.8% agarose gel and the 7 kb non-stuffer pLKO.1 band was excised and gel purified. The gel purification process was performed using GF-1 gel DNA recovery kit and the DNA was eluted in 30 µL of autoclaved distilled water. Agarose gel analysis of the gel purification products was then performed to check for the plasmid yield of gel purification.

Table 3.10: Reaction mixture for simultaneous dual digestion of lentiviral plasmid pLKO.1 using *AgeI* and *EcoRI*.

Component	Concentration
plasmid pLKO.1	6 µg
10 × Buffer O	1 ×
<i>AgeI</i>	30 U
<i>EcoRI</i>	30 U
Autoclaved ddH ₂ O	top up to 50 µL

3.7.5 Ligation and Transformation into Competent Cells

To clone the annealed oligonucleotides into pLKO.1, ligation mixtures as shown in Table 3.11 were prepared. To monitor the efficiency of ligation, mixture for ligation positive control was prepared according to the proportion of the mixture as shown in Table 3.11, however, *AgeI*-linearized pLKO.1 TRC was included to replace the non-stuffer pLKO.1 and the annealed oligonucleotides was excluded. To monitor vector self-ligation, mixture for

ligation negative control was prepared according to the proportion of the mixture as shown in Table 3.11, however, the annealed oligonucleotides was excluded. The ligation mixtures were incubated in ice-water bath overnight. Eight microliters of ligation mixture was transformed into 100 μL of competent *E.coli* DH5 α and JM109 cells using heat shock method as described in Section 3.4.1. The transformation reactions were plated on LB ampicillin agar plates and incubated overnight at 37 $^{\circ}\text{C}$ to allow the growth of transformed colonies.

Table 3.11: Ligation mixture for cloning of annealed oligonucleotides into non-stuffer lentiviral plasmid pLKO.1 in generation of shRNA constructs.

Component	Volume
Annealed oligonucleotides	2 μL
Non-stuffer pLKO.1	1 μL
10 \times ligase buffer with 10 mM ATP	2 μL
T4 DNA ligase (400 U/ μL)	1 μL
Autoclaved ddH ₂ O	top up to 20 μL

3.7.6 Plasmid Extraction, Screening of shRNA Inserts and Sequencing

Since lentiviral plasmid pLKO.1 TRC is low-copy-number vector, to compensate for this, larger volume of LB ampicillin broth was used to grow the transformed colony for subsequent minipreparation. A well-isolated transformed colony on transformation plate obtained from process as elaborated in Section 3.7.5 was inoculated into 10 mL of LB ampicillin broth and incubated overnight at 37 °C with shaking at 200 rpm. The minipreparation was proceed using the method described in Section 3.6.3. To screen for shRNA insert, simultaneous restriction digestion of purified plasmids with *EcoRI* and *NcoI* was performed and the reaction mixture was then electrophoresed on 1% agarose gel to visualize the digestion products. For digestion of positive clone, a 2 kb band and a 5 kb band should be seen under UV illumination. After that, the purified plasmid for positive clone would be sent to 1st BASE Laboratories Sdn Bhd, Selangor, Malaysia for sequencing with pLKO.1 sequencing primer (5'-CAAGGCTGTTAGAGAGATAATTGGA-3'). Due to the strong potential of shRNA insert in forming secondary loop structure which often causes sequencing difficulty, difficult template sequencing service (SS1006) provided by the company was ordered.

CHAPTER 4

RESULTS

4.1 Competency Test for Self Prepared Chemical Competent Cells

Transformation of competent *E. coli* DH5 α with plasmid (pcDNATM3.1D/V5-His-TOPO WT α -syn) yielded approximately 580 colonies after 16 hours incubation at 37 °C as shown in Figure 4.1.

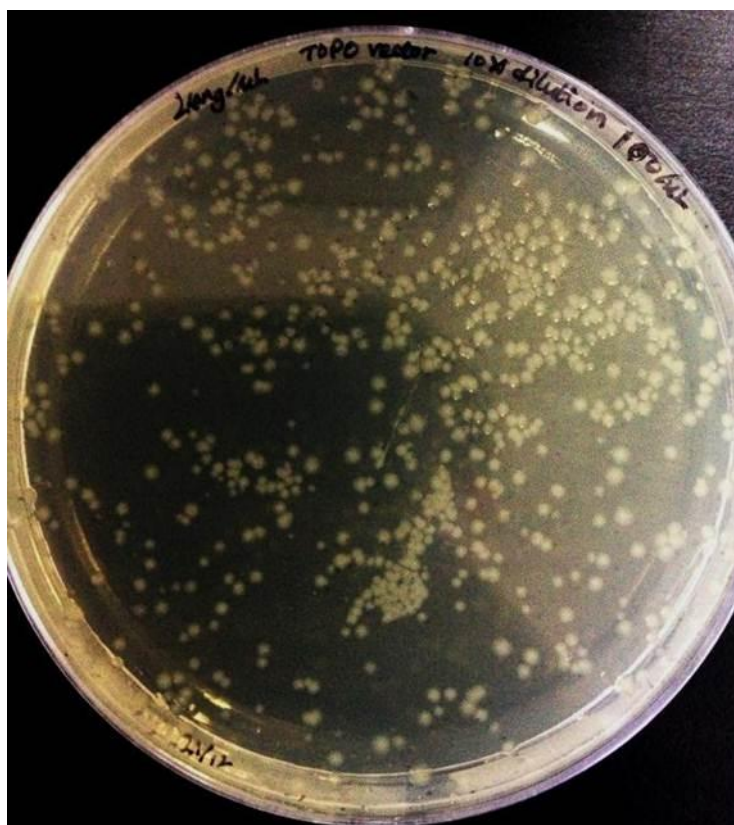


Figure 4.1: Self-prepared chemical competent *E. coli* DH5 α transformed with pcDNATM3.1D/V5-His-TOPO WT α -syn on LB ampicillin agar plate.

Since 1 μL of plasmid (pcDNATM3.1D/V5-His-TOPO WT α -syn) with the concentration of 24 ng/ μL was used, and the dilution factor used was 100, the competency of *E.coli* DH5 α could be calculated using the formulae shown in Section 3.4.2. The calculated cell competency was 2.417×10^6 cfu/ μg plasmid.

Chemical competent cells normally yield 10^6 to 10^7 transformants (Sambrook and Russell 2001; Invitrogen 2007), which would allow routine cloning experiments to be easily performed. Since the self-prepared competent cells met this range of transformation efficiencies, subsequent site-directed mutagenesis and shRNA cloning in this study were continued.

4.2 Propagation of Plasmid Template in Dam+ Dcm+ *E.coli*

4.2.1 Plasmid Extraction (Midipreparation)

Midipreparation was performed on one of the colonies on the agar plate as shown in Figure 4.1. Midipreparation yielded plasmid DNA (pcDNATM3.1D/V5-His-TOPO WT α -syn) which was dissolved in 50 μL of TE buffer. Data obtained from nano-spectrophotometry analysis of the purified plasmid is shown in Table 4.1. Pure plasmid should have purity within the range of 1.8 to 2.0. Hence, the purified plasmid (midipreparation) was pure enough and suitable to be template for subsequent PCR process.

Table 4.1: Nano-spectrophotometry analysis showing A_{260} , A_{280} , purity and concentration of the purified plasmid DNA (midipreparation).

Parameter	Value
A_{260}	0.970
A_{280}	0.527
Purity (A_{260}/A_{280})	1.849
Concentration (ng/ μ L)	2412

4.2.2 Confirmation of Purified Plasmid using *Xho*I Linearization

The total size of pcDNATM3.1D/V5-His-TOPO WT α -syn is 5937 bp (backbone size: 5514 bp; full-length wild type human α -syn gene: 423 bp).

Linearization of purified plasmid (midipreparation) using *Xho*I yielded a band with size of approximately 6 kb as shown in Figure 4.2.

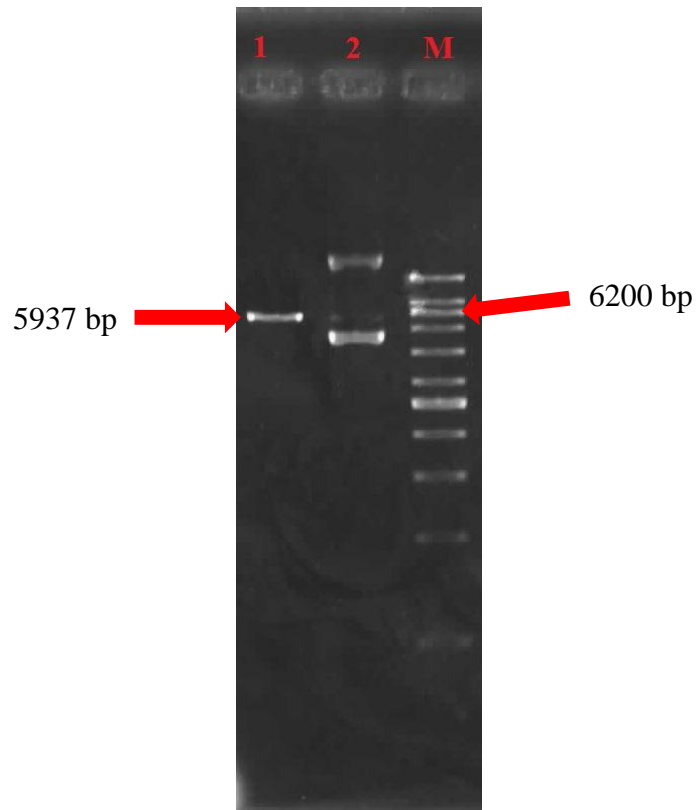


Figure 4.2: Electrophoresis gel (1% agarose) image showing migration of linearized and unlinearized purified plasmid (midpreparation). Lane 1: Linearized purified plasmid (midpreparation). Lane 2: Unlinearized purified plasmid (midpreparation). Lane M: 1kb DNA Ladder.

4.3 Mutant Strand Synthesis

4.3.1 Transformation and Plasmid Extraction (Minipreparation)

Several attempts on transformation of post-*DpnI*-treated PCR (QCM) products into competent DH5 α stored in 16 % glycerol at -80 °C for about 20 days yielded no colony. It was suspected that the competent cells stored in glycerol stock lost their competency due to prolonged storage period.

Transformation of post-*DpnI*-treated PCR (QCM) products into freshly prepared competent DH5 α yielded colonies on the LB-ampicillin agar plate.

Retransformation of the same DNA products into same batch of competent DH5 α which had been stored back to 4°C for 22 hours (within 12-24 hours) after preparation also yielded colonies on the LB-ampicillin agar plate. Table 4.2 shows the number of colonies obtained using QCM with DH5 α as transformation host.

Table 4.2: Number of colonies, screened colonies and mutant obtained using Stratagene QuickChangeTM Site-Directed Mutagenesis Protocol (QCM) with DH5 α as the transformation host.

Construct	DH5 α					
	*Fresh			*Stored (12-24 hours)		
	Colonies	Screened	Mutant	Colonies	Screened	Mutant
S87A	3	3	0	4	3	0
S87D	3	3	0	3	3	0
S129A	2	2	0	0	0	0
S129D	4	3	0	10	3	0

* Fresh refers to transformation into freshly-prepared competent cells, Stored (12-24 hours) refers to retransformation of same DNA products into same batch of competent cells within 12-24 hours.

Transformation of post-*DpnI*-treated PCR (SPRINP) products into freshly prepared competent DH5 α and JM109 yielded colonies on LB-ampicillin agar plate. Retransformation of the same DNA products into same batch of competent DH5 α and JM109 which had been stored back to 4°C for 22 hours (within 12-24 hours) after preparation also yielded colonies on the LB-

ampicillin agar plate. Table 4.3 and 4.4 show the number of colonies obtained using SPRINP with DH5 α and JM109 as transformation host respectively.

Table 4.3: Number of colonies, screened colonies and mutant obtained using Single Primer Reaction In Parallel (SPRINP) with DH5 α as the transformation host.

Construct	DH5 α					
	*Fresh			*Stored (12-24 hours)		
	Colonies	Screened	Mutant	Colonies	Screened	Mutant
S87A	3	3	0	1	1	0
S87D	1	1	0	2	2	0
S129A	1	1	0	1	1	0
S129D	1	1	0	1	1	0

* Fresh refers to transformation into freshly-prepared competent cells, Stored (12-24 hours) refers to retransformation of same DNA products into same batch of competent cells within 12-24 hours.

Table 4.4: Number of colonies, screened colonies and mutant obtained using Single Primer Reaction In Parallel (SPRINP) with JM109 as the transformation host.

Construct	JM109					
	*Fresh			*Stored (12-24 hours)		
	Colonies	Screened	Mutant	Colonies	Screened	Mutant
S87A	5	2	0	7	2	0
S87D	10	2	0	44	2	0

Table 4.4 (continued):

Construct	JM109					
	*Fresh			*Stored (12-24 hours)		
	Colonies	Screened	Mutant	Colonies	Screened	Mutant
S129A	1	1	0	0	0	0
S129D	3	2	0	2	2	0

* Fresh refers to transformation into freshly-prepared competent cells, Stored (12-24 hours) refers to retransformation of same DNA products into same batch of competent cells within 12-24 hours.

Minipreparation was performed for all the colonies on the plates. The concentration of the purified plasmid ranged from 85 ng/ μ L to 350 ng/ μ L. The purity (A_{260}/A_{280}) of the plasmid (minipreparation) ranged from 1.5 to 2.0. Low A_{260}/A_{280} ratio of some of the purified samples might be due to low concentration of nucleic acid in the sample itself (Thermo Scientific, n.d.). The best way to determine the DNA quality is based on the functionality of downstream process. Hence, subsequent procedures were continued.

4.3.2 Screening using *Xho*I Linearization and Sequencing

All the purified plasmids (minipreparation) were screened using *Xho*I digestion before sending for sequencing. 6 kb band was observed on gel after overnight digestion with *Xho*I as shown in Figure 4.3. The band size matched to the linearized pcDNATM3.1D/V5-His-TOPO WT α -syn (midipreparation) on Lane 2. However, it could not distinguish between wild type gene and

mutant gene. All the purified plasmid (minipreparation) showed positive result in *XhoI* screening and were sent for sequencing.



Figure 4.3: Electrophoresis gel (1% agarose) image showing the screening of purified plasmid (minipreparation) using *XhoI* linearization before sequencing. Lane M: 1 kb DNA Ladder. Lane 1: Linearized pcDNATM3.1D/V5-His-TOPO WT α -syn (midipreparation). Lane 2: Linearized purified plasmid (minipreparation). Lane 3: Unlinearized purified plasmid (minipreparation).

There was no overlapping peak in the sequencing chromatograms for the purified plasmids as shown in Figure 4.4 (S87D mutant construct) and Figure 4.6 (S129D mutant construct). This indicated that the purified plasmids (minipreparation) were clean and there was no mixed plasmid population.

Sequence alignments between purified plasmid and wild type human α -syn to check for nucleotide substitution at diversified region were shown in Figure 4.5 (codon 87) and Figure 4.7 (codon 129). None of the sequencing results showed desired mutant constructs (S87A, S87D, S129A and S129D), instead all appeared to be wild type.

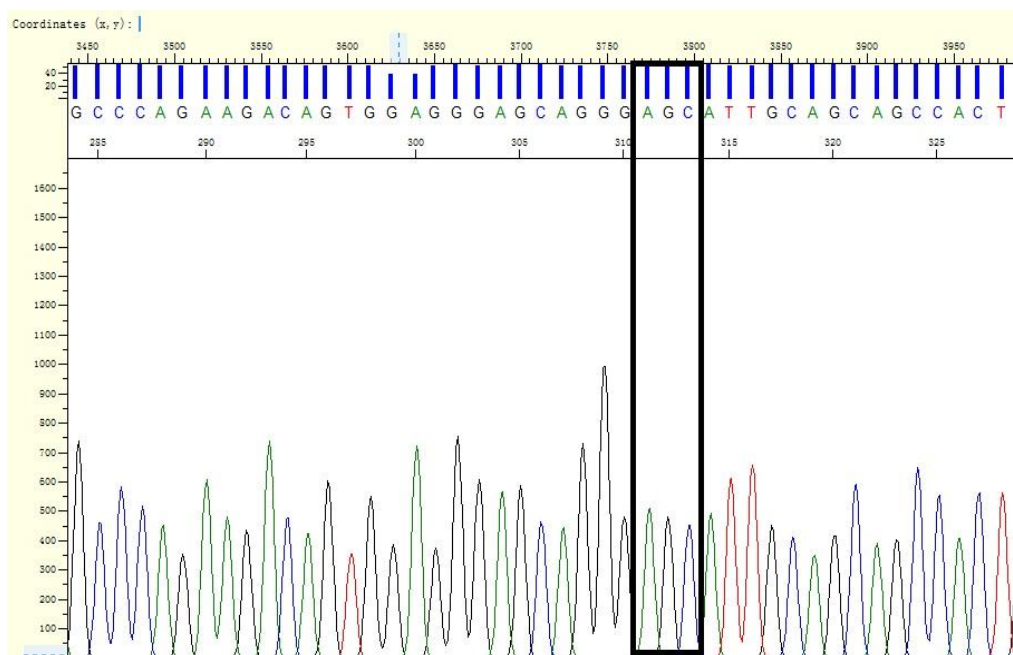


Figure 4.4: Sequencing chromatogram of purified plasmid (minipreparation) in S87D mutant construction. Serine (AGC) at codon 87 of full-length human wild type α -syn remained unchanged.

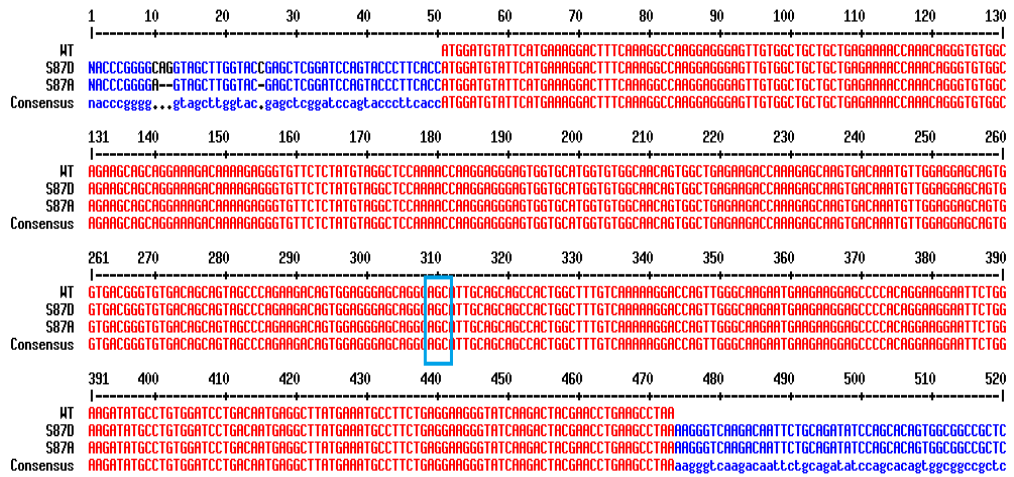


Figure 4.5: Sequence alignment between purified plasmid (miniprep) for S87A and S87D mutant constructions and full-length wild type human α -syn (GenBank ID: BC108275.1) cDNA (Clone ID: 6147966). MultAlin Multiple Sequence Alignment Online Program available at <http://multalin.toulouse.inra.fr/multalin> was used to perform the alignment. Serine (AGC) at codon 87 of α -syn remained unchanged.

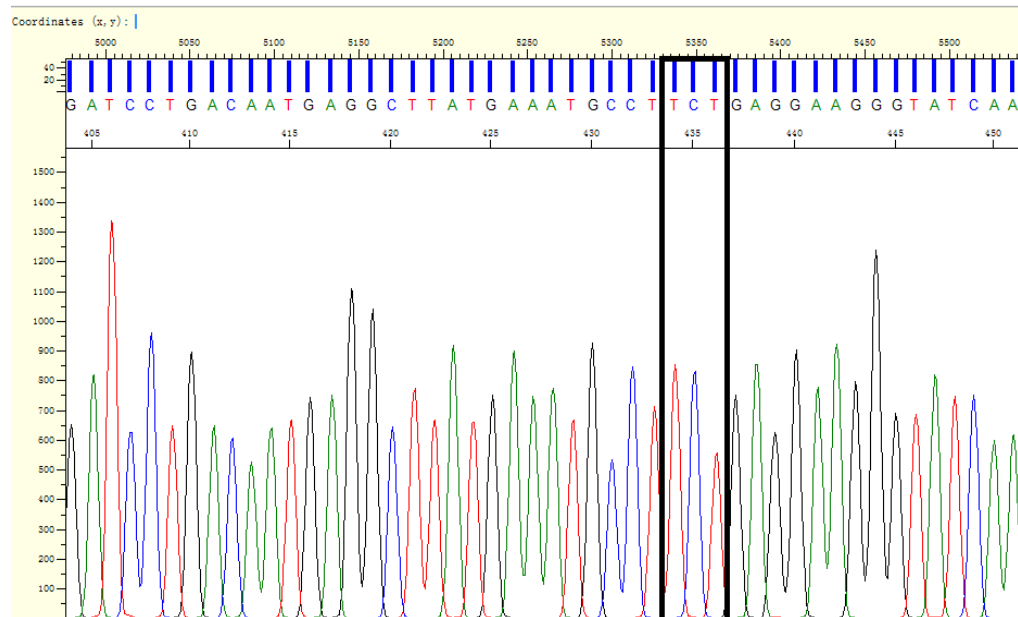


Figure 4.6: Sequencing chromatogram of purified plasmid (miniprep) in S129D mutant construction. Serine (TCT) at codon 129 of full-length human wild type α -syn remained unchanged.

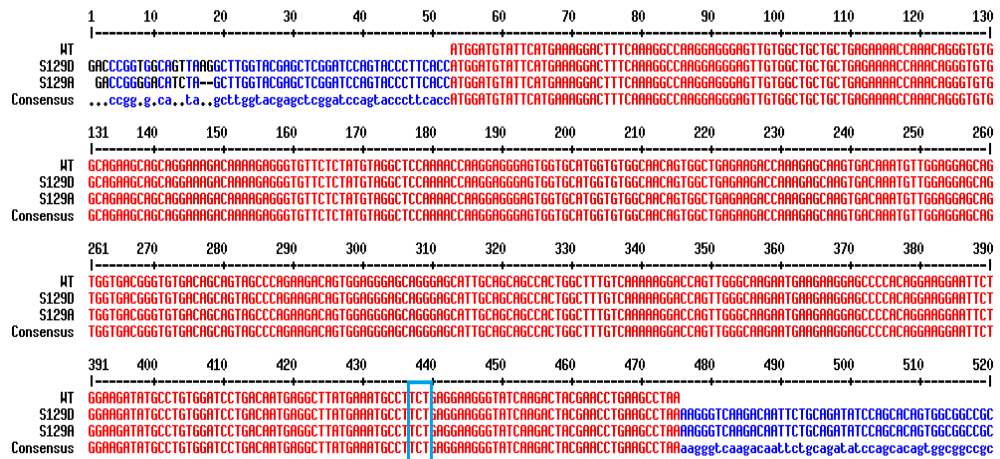


Figure 4.7: Sequence alignment between purified plasmid (minipreparation) for S129A and S129D mutant constructions and full-length wild type human α -syn (GenBank ID: BC108275.1) cDNA (Clone ID: 6147966). MultAlin Multiple Sequence Alignment Online Program available at <http://multalin.toulouse.inra.fr/multalin> was used to perform the alignment. Serine (TCT) at codon 129 of α -syn remained unchanged.

4.3.3 Troubleshooting

Post-*DpnI*-treated PCR products for both QCM and SPRINP methods were electrophoresed on 1% agarose gel at 90 V for 40 minutes. The electrophoresis outcomes for the former and latter were shown in Figure 4.8 and Figure 4.9 respectively.

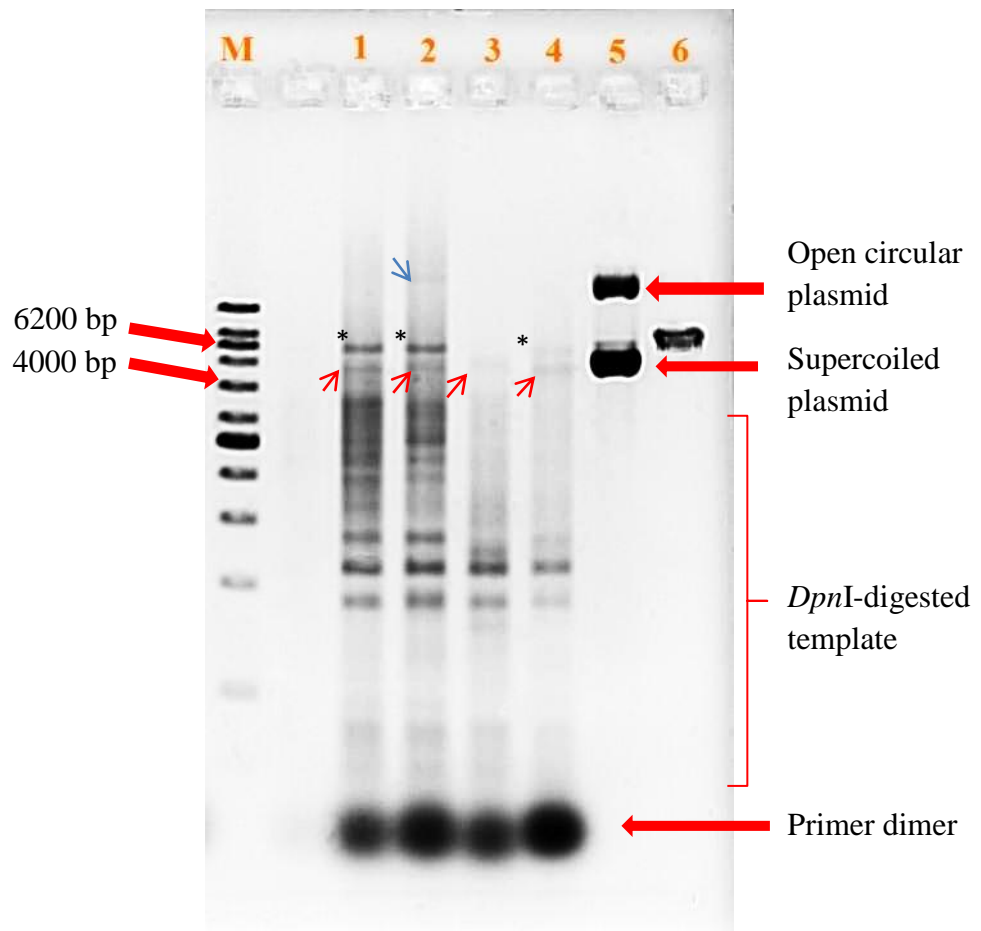


Figure 4.8: Electrophoresis gel (1% agarose) image showing migration of post-*DpnI*-treated PCR (QCM) products. Lane M: 1 kb DNA ladder. Lane 1: Post-*DpnI*-treated PCR (QCM) product for S129D. Lane 2: Post-*DpnI*-treated PCR (QCM) product for S129A. Lane 3: Post-*DpnI*-treated PCR (QCM) product for S87D. Lane 4: Post-*DpnI*-treated PCR (QCM) product for S87A. Lane 5: Unlinearized pcDNATM3.1D/V5-His-TOPO WT α -syn (midipreparation). Lane 6: Linearized pcDNATM3.1D/V5-His-TOPO WT α -syn (midipreparation).

In Figure 4.8, there were faint bands (indicated by red thin arrow) on Lanes 1, 2, 3 and 4 which migrated at the same distance with the supercoiled form of the unlinearized pcDNATM3.1D/V5-His-TOPO WT α -syn on Lane 5. There was also single faint band (indicated by blue thin arrow) on Lane 2 which migrated at same distance with open circular form of the unlinearized plasmid

on Lane 5. Bands which migrated at the same distance with the linearized pcDNATM3.1D/V5-His-TOPO WT α -syn on Lane 6 (indicated by asterisk) were observed on lanes 1, 2 and 4 but not on Lane 3. This could imply very little or no PCR amplification on Lane 3. Many discrete bands with molecular weight of approximately below 4000 bp which indicated *DpnI*-digested template were observed on Lanes 1, 2, 3 and 4. Primer dimers were also observed on Lanes 1, 2, 3 and 4 at the bottom of the gel.

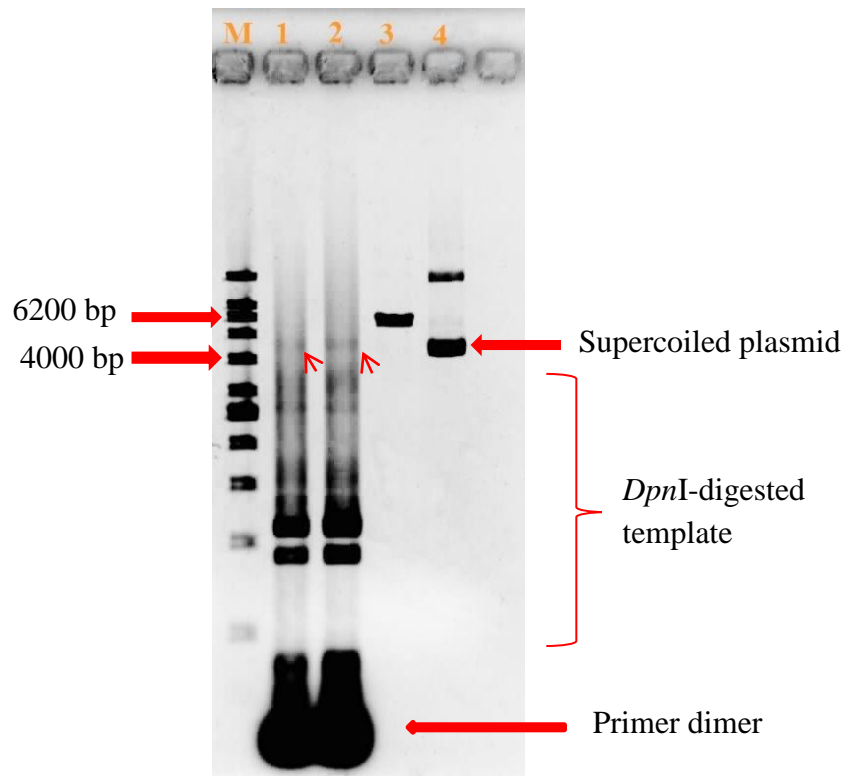


Figure 4.9: Electrophoresis gel (1% agarose) image showing migration of post-*DpnI*-treated PCR (SPRINP) products. Lane M: 1 kb DNA ladder. Lane 1: Post-*DpnI*-treated PCR (SPRINP) products for S129D. Lane 2: Post-*DpnI*-treated PCR (SPRINP) products for S129A. Lane 3: Linearized pcDNATM3.1D/V5-His-TOPO WT α -syn (midpreparation). Lane 4: Unlinearized pcDNATM3.1D/V5-His-TOPO WT α -syn (midpreparation).

In Figure 4.9, there were faint bands (indicated by red thin arrow) on Lane 1 and Lane 2 which migrated at the same distance with the supercoiled form of the unlinearized pcDNATM3.1D/V5-His-TOPO WT α -syn on Lane 4. Bands which migrated at the same distance with linearized pcDNATM3.1D/V5-His-TOPO WT α -syn on Lane 3 was not observed on Lane 1 and Lane 2. This could imply very little or no PCR amplification. Many discrete bands with molecular weight of approximately below 4000 bp which indicated *DpnI*-digested template were observed on Lane 1 and Lane 2. Primer dimers were also observed on Lane 1 and Lane 2 at the bottom of the gel.

4.4 Generation of γ -syn Gene Silencing Constructs

4.4.1 Dual Digestion of Lentiviral Plasmid pLKO.1 TRC

Dual digestion of lentiviral plasmid pLKO.1 TRC with 30 U of *AgeI* and 30 U of *EcoRI* yielded two bands which could be observed under UV illumination on gel. One band was approximately 7 kb in size while the other was approximately 1.9 kb in size. The 7 kb band for non-stuffer pLKO.1 TRC plasmid DNA was excised and gel purified. Subsequent agarose gel analysis of gel purification products revealed a thick band with the size of approximately 7 kb as shown in Figure 4.10. Due to inability to check whether the sticky ends had been removed properly and there was no other band on the same gel, it was assumed that there was proper digestion. Thus, the subsequent procedures were continued.

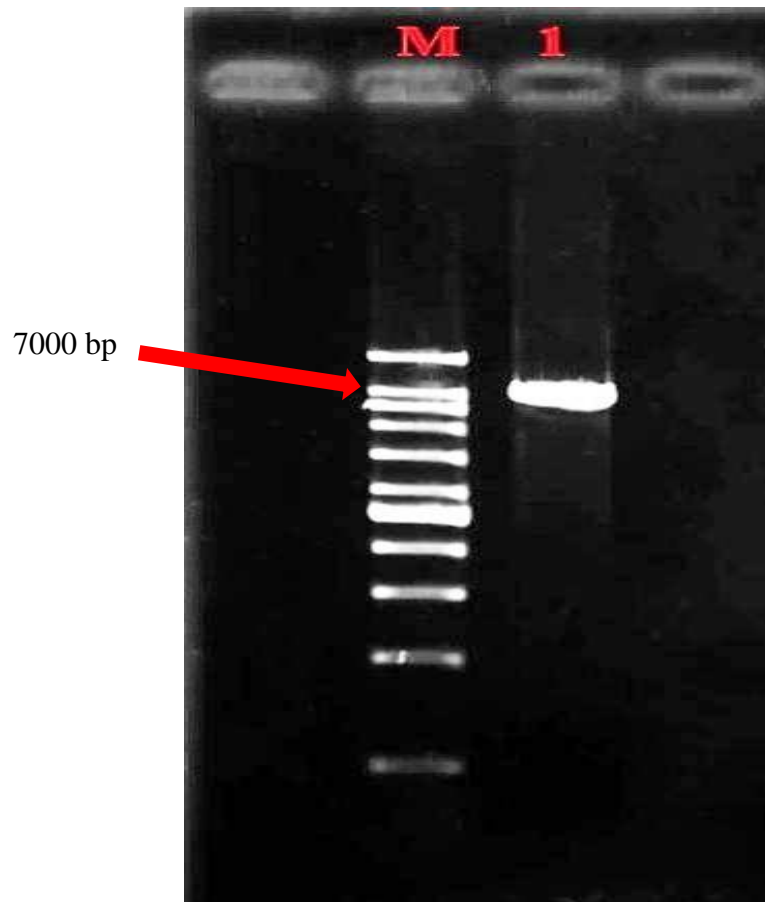


Figure 4.10: Electrophoresis gel (1% agarose) image showing migration of gel purification product for non-stuffer pLKO.1 TRC. Lane M: 1 kb DNA ladder. Lane 1: Gel purification product for non-stuffer pLKO.1 TRC.

4.4.2 Efficiency of shRNA Oligonucleotides Annealing

After annealing the forward and reverse oligonucleotides for γ -syn shRNA 1, γ -syn shRNA 2 and γ -syn shRNA 3, the efficiency of annealing was checked by electrophoresing the annealed oligonucleotides on 3% agarose gel at 80 V for 50 minutes. The electrophoresis gel image is shown in Figure 4.11.

For efficient annealing of oligonucleotides, the upper band (~ 50 bp) on Lanes 2, 3 and 4 should be thicker as compared to lower band (~ 25 bp). Since the upper bands (representing dimer) appeared to be thinner than lower bands, the annealing efficiency was suspected to be suboptimal. The upper band on lane 1 appeared to be thicker as compared to lower band. This could be due to the self-dimer of forward oligonucleotides or reverse oligonucleotides instead of the proper annealing between these two forward and reverse species.

All the attempts on oligonucleotides annealing gave same migration pattern as shown in Figure 4.11, which could possibly lower down the chances of success of subsequent ligation steps.

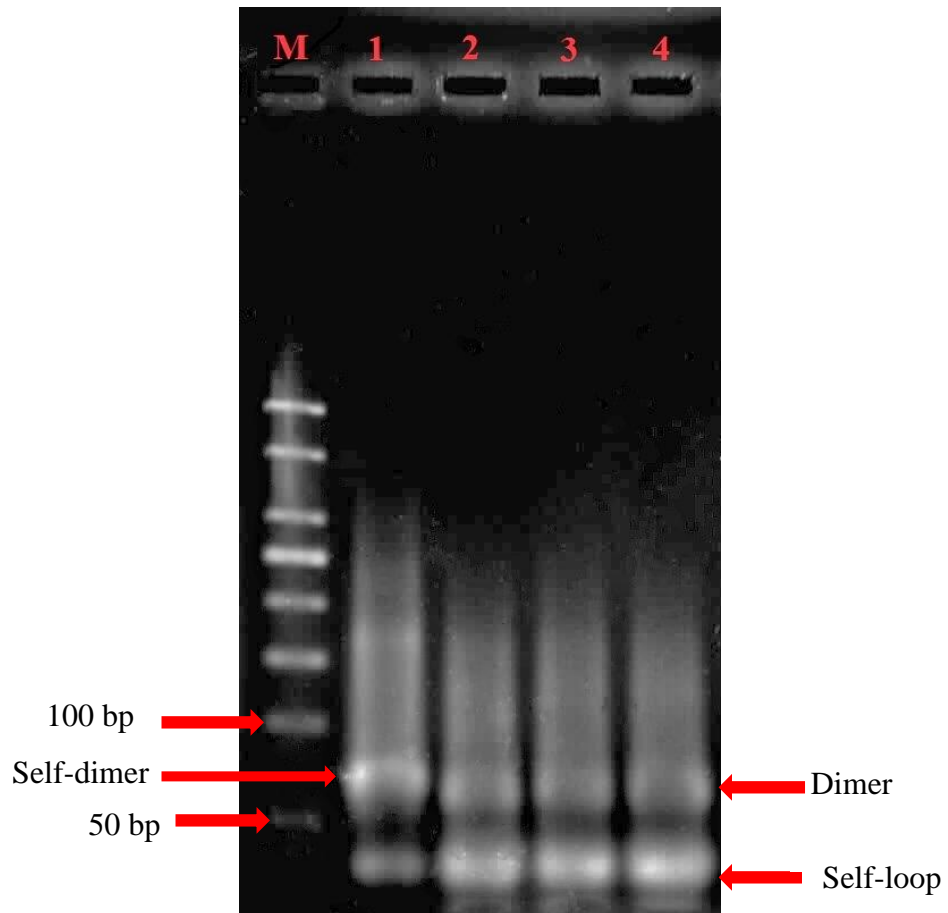


Figure 4.11: Electrophoresis gel (3% agarose) image showing the annealing efficiency test of shRNA oligonucleotides. Lane M: 50 bp DNA ladder. Lane 1: Mixture of forward and reverse oligonucleotides before annealing. Lane 2: Oligonucleotides for γ -syn shRNA 1 after annealing. Lane 3: Oligonucleotides for γ -syn shRNA 2 after annealing. Lane 4: Oligonucleotides for γ -syn shRNA 3 after annealing.

4.4.3 Gel Analysis of Ligation Products

After ligation, the ligation products for γ -syn shRNA 1, γ -syn shRNA 2 and γ -syn shRNA 3 were electrophoresed on 1% agarose gel at 90 V for 40 minutes. The electrophoresis outcome is shown in Figure 4.12. There was mobility shift of band for all the three constructs on Lanes 1, 2 and 3 respectively as compared to the non-stuffer pLKO.1 TRC on Lane 4. This may indicate that

ligation of three shRNA annealed oligonucleotides with the non-stuffer pLKO.1 TRC worked. shRNA oligonucleotides which did not involve in the ligation reaction were observed at the bottom of the gel. Although the electrophoresis was over-run, the information about the ligation reaction still could be obtained.

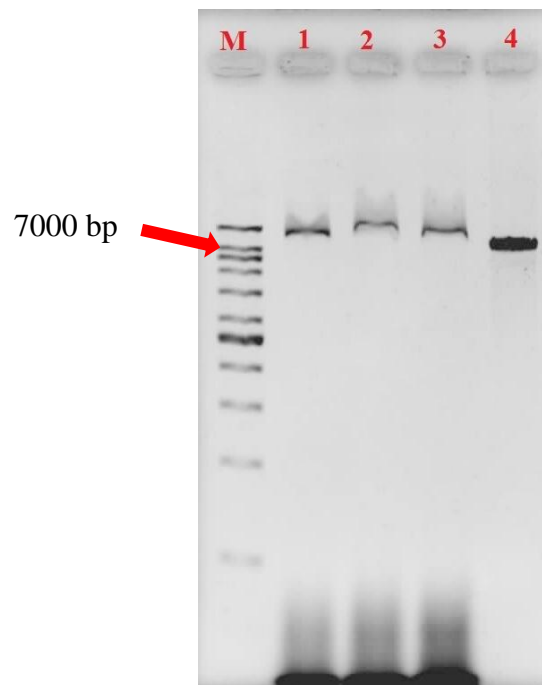


Figure 4.12: Electrophoresis gel (1% agarose) image showing migration of ligation products and non-stuffer pLKO.1 TRC. Lane M: 1 kb DNA ladder. Lane 1: Ligation product for γ -syn shRNA 1. Lane 2: Ligation product for γ -syn shRNA 2. Lane 3: Ligation product for γ -syn shRNA 3. Lane 4: Non-stuffer pLKO.1 TRC.

4.4.4 Transformation of Ligation Product and Plasmid Extraction

Several attempts on transformation of ligation products (γ -syn shRNA 1, 2 and 3) into freshly-prepared chemical competent *E. coli* DH5 α and JM109 yielded no colony. There was also growth of colonies on the plates for ligation positive control. No colony grew on the plates for ligation negative control. The final attempt of transformation using DH5 α and JM109 as transformation hosts, three colonies were obtained for γ -syn shRNA 3 of which two colonies belonged to DH5 α and the other one belonged to JM109. Table 4.5 shows the nano-spectrophotometry analysis of the plasmid purified from these three colonies.

Table 4.5: Nano-spectrophotometry analysis showing the A260, A280, purity and concentration of plasmid (Clone 1, Clone 2 and Clone 3) purified from transformed colonies for γ -syn shRNA 3.

	JM109	DH5 α	
	Clone 1	Clone 2	Clone 3
A260	2.108	1.126	1.784
A280	0.843	0.630	0.962
Purity (A260/A280)	2.500	1.790	1.860
Concentration (ng/μL)	105.4	56.3	89.2

4.4.5 Screening of shRNA Inserts and Sequencing

Dual digestions of purified plasmid samples (Clone 1, Clone 2 and Clone 3) were performed using 10 U of *EcoRI* and 10 U of *NcoI* for three hours at 37 °C. The digestion products were electrophoresed on 1% agarose gel at 90 V for 40 minutes. The electrophoresis outcome was shown in Figure 4.13.

In Figure 4.13, dual digestion of the purified plasmids (clone 1-3) produced four bands as shown on Lane 4-6 of which this deviated from the expected bands pattern for positive clone. Three conformations including supercoiled, linear and open circular form of the unlinearized purified plasmids could be observed as shown on Lane 1-3. The molecular weight of bands for linear form of the three purified plasmids appeared to be approximately 5200 bp which may indicate the size of the purified plasmids. Although unexpected bands pattern was obtained, one of the purified plasmid samples (Clone 3) was still sent for sequencing to aid troubleshooting. However, sequencing of the purified plasmid using pLKO.1 sequencing primer was unsuccessful.

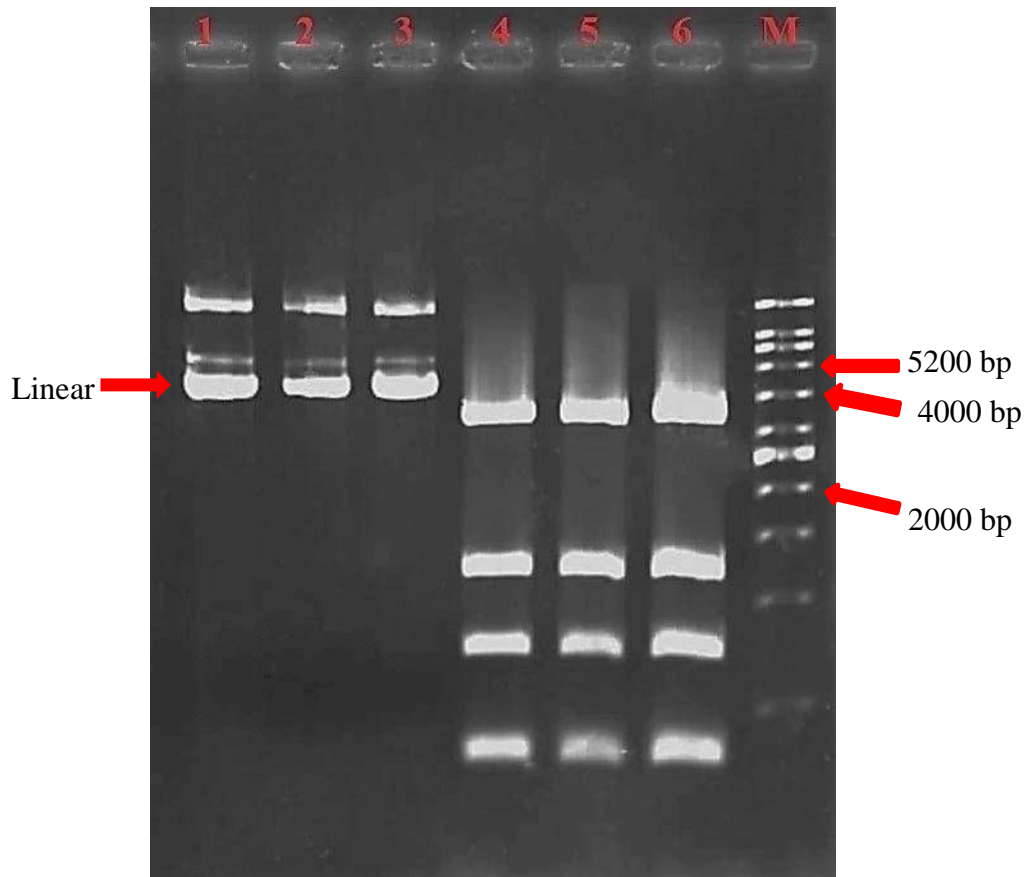


Figure 4.13: Electrophoresis gel (1% agarose) image showing migration of unlinearized purified plasmid and the respective dual digested products in the screening of shRNA insert for γ -syn shRNA 3. Lanes 1-3: Purified plasmid from Clone 1, Clone 2 and Clone 3. Lanes 4-6: Dual digested products corresponding to purified plasmid on Lanes 1-3 following the sequence. Lane M: 1 kb DNA ladder.

CHAPTER 5

DISCUSSION

5.1 Generation of α -syn Phosphorylation Mutant Constructs

5.1.1 Competent Cells

Competency of self-prepared chemical competent cells (DH5 α) used in this study achieved 2.417×10^6 cfu/ μ g plasmid. Competence is described as the physiological state of cells which allow them to uptake the exogenous DNA molecules. Although transformation using chemical method is routinely applied for molecular biology purposes, the mechanism behind it remained poorly understood. It was postulated that the bivalent cation like Mg²⁺ and Ca²⁺ could bound to membrane phospholipid and make them positively-charged which in turn attract the negatively-charged DNA to stick to the membrane. Subsequent heat shock would provide energy and help in faster uptake of DNA into the cells (Singh et al., 2010).

Competency of the self-prepared competent cells in this study met the range of transformation efficiency ($10^6 - 10^7$ cfu/ μ g plasmid) required for routine cloning experiment (Sambrook and Russell 2001; Invitrogen 2007). Different form of plasmid would give different transformation efficiency. Supercoiled or intact plasmid generally transform better (more than hundred fold) than linearized form of plasmid possibly due to smaller in size and circular conformation resulting in higher resistance to intracellular nucleases activity (Sambrook and Russell 2001; Zheng et al., 2004). This explained the difficulty

in transforming linearized amplification product of SDM (Ling and Robinson 1997; Edelheit et al., 2009) to the competent cells. Hence, high competent cells achieving transformation efficiency of 10^7 to 10^9 cfu/ug plasmid which are more commonly available commercially would be the best for SDM (Laible and Boonrod 2009) especially when the amplification efficiency is not ideal as occurred in this study.

Several attempts on transformation of post-*DpnI*-PCR product using competent cells stored in glycerol stock for more than 20 days failed to produce any colony. In contrast, transformation using freshly prepared competent cells and competent cells which had been stored for 12-24 hours at 4 °C successfully produced a few colonies. Chemical competent cell preparation is a tedious process and competency could be affected by many factors including storage duration (Tu et al., 2005). Tu et al. (2005) reported reduction of transformation efficiency using competent cells stored for more than 15 days at -70 °C. Besides, it was also reported that freshly prepared competent cells which had been stored for 12-24 hours at 4 °C could achieve four to six fold increase of transformation efficiency than original level (Sambrook and Russell 2001). However, in this experiment there was no obvious difference in transformation efficiency (in term of number of colonies recovered after transformation) between freshly prepared competent cells and competent cells which had been stored for 12-24 hours at 4 °C. Competent cells are known to be fragile and their competency could reduce due to multiple freeze-thaw cycle (Sundquist and Doers 1998; Tu et al., 2005). In this study, the freshly prepared competent cells were stored back to 4 °C after

transformation and used to transform again after 22 hours. Hence, the cells may be exposed to variation of temperature during transformation immediately after preparation, which may render certain population of cells to die and, thus could not achieve expected increase in transformation efficiency after 12-24 hours.

5.1.2 Propagation of Plasmid Template in dam^+ dcm^+ *E. coli*

Plasmid pcDNATM3.1D/V5-His-TOPO WT α -syn was successfully propagated in and purified from dam^+ *E. coli* DH5 α . It was essential to use plasmid purified from *E. coli* cells which constitutively express the deacetylmethyltransferase (Dam) as the template in subsequent PCR process. This would allow subsequent destruction of wild type plasmid template using *DpnI*, while enriching the amplified mutant product before transformation (Zawaira et al., 2012).

TE buffer was used to dissolve the purified plasmid (midpreparation) because it contains EDTA which could serve as chelator of divalent ions like Mg^{2+} , thus inhibiting activity of possible contaminating nuclease. Since EDTA may inhibit downstream enzymatic process, aliquot of purified plasmid was first diluted using autoclaved distilled water with dilution factor of 100 before linearized with *XhoI* and used as template in subsequent PCR.

Electrophoresis of *XhoI*-linearized product yielded single band with size of approximately 6 kb as shown on Lane 1 in Figure 4.2. This matched with the

expected size of pcDNATM3.1D/V5-His-TOPO WT α -syn (5937 bp), further confirming that the purified plasmid was suitable to be template of subsequent PCR amplification of mutant. The unlinearized purified plasmid (Lane 2 in Figure 4.2) composed of three forms: supercoiled (bottom), linear (middle) and open circular (top). Supercoiled plasmid migrated much faster than linearized and open circular form of plasmid on gel because it is more compact and thus receiving less resistance during migration. Absence of supercoiled and open circular form of plasmid on Lane 1 in Figure 4.2 indicated complete digestion of the purified plasmid.

5.1.3 Inefficient Mutant Strand Synthesis

5.1.3.1 Stratagene QuickChangeTM Site-Directed Mutagenesis Protocol

Sequencing results showed that none of the plasmid purified (miniprep) from colonies obtained using QCM method was mutant constructs (S87A, S87D, S129A and S129D). Electrophoresis outcomes of post-*DpnI*-treated PCR products showed very little or no amplification of PCR product for S87D construct as shown in Figure 4.8.

Although there were bands (indicated by asterisk) migrating at the same distance with linearized plasmid for S87A, S129A and S129D mutant constructs using QCM method as shown in Figure 4.8, they could not indicate significant amplification. The possibility that the linearized bands were originated from PCR template could not be excluded, since the purified plasmid (pcDNATM3.1D/V5-His-TOPO WT α -syn) used as PCR template also

contained some proportion of linearized plasmid as shown on Lane 5 in Figure 4.8. Low yield of amplification products (linearized plasmid) may not be recovered via subsequent transformation process since the competency of competent cells used in this study was not ideally high which had been discussed earlier in Section 5.1.1.

Although QCM method appeared to be simple and straightforward in creating desired mutation, some researchers reported difficulty in generating desired mutant using this method (Wang and Malcolm 1999; Fang 2004; Zheng et al., 2004; Liu and Naismith 2008). As elaborated earlier in Section 2.4, QCM method has two major disadvantages which are high potential for primer dimer formation due to the use of complementary primer pairs as well as relatively low amplification efficiency. These two may contribute to the failure in generating α -syn mutants using QCM method in this study.

5.1.3.2 Single Primer Reaction in Parallel

To reduce the problem of primer dimer due to complete complementarity when using QCM method, SPRINP method was used instead to generate mutants. However, this method also failed to generate mutants (S87A, S87D, S129A and S129D). Absence of linear full-sized amplification band with molecular weight of approximately 6000 bp as shown in Figure 4.9 could imply low amplification efficiency or no amplification.

There were several potential factors which could contribute to low or no amplification when using SPRINP method. First, annealing of primer to the target site on plasmid template might be outcompeted by the completely matched wild-type duplex at the diversified region (Wang and Malcolm 1999). When primer-template annealing does not happen, subsequent extension could not happen. Second, the primer pool available for annealing with template at the target site was significantly reduced due to formation of homo-dimers. Homo-dimer analysis using online oligonucleotide analysis tool OligoAnalyzer 3.1 available at <http://eu.idtdna.com/analyzer/applications/oligoanalyzer/> (results shown in Appendix B) showed that the primers used for S87A, S87D, S129A and S129D constructs could produce significant homo-dimers with Delta G value lesser than -6 kcal/mole (Sigma-Aldrich n.d.).

Third, the conformation of the plasmid template may be too supercoiled and the denaturation duration (2 minutes) during PCR thermal cycling may be too short to “denature” them. Hence, even after uncoiling of supercoiled conformation and subsequent unwinding of double helix during initial denaturation and denaturation stage of thermal cycling, the plasmid template may re-anneal and re-coil back immediately once the temperature dropped during annealing stage of thermal cycling (Fang 2004). These events may happen too quickly, reducing the chance of primer-template annealing. Dorrell et al. (1996) also reported that closed circular DNA could be less efficient template for amplification than alkaline-denatured plasmid which most probably contained open circular plasmid DNA and linear plasmid DNA. It is

also possible that combination of these three potential factors led to low or no amplification.

5.1.4 Incomplete *DpnI* Selection

Most approaches to SDM including those applying *DpnI* selection could not eliminate completely the wild type template (Wang and Malcolm 1999; Goldsmith et al., 2007). Sequencing results showed that all the purified plasmids (minipreparation) were wild type α -syn constructs. Electrophoresis outcomes of the post-*DpnI*-treated PCR products revealed single bands which migrated at the same distance with the supercoiled form and open circular form of plasmid template (pcDNATM3.1D/V5-His-TOPO WT α -syn) as shown in Figure 4.8 and Figure 4.9. This may imply incomplete *DpnI* digestion of the parental plasmid template in PCR, since the newly synthesized mutant PCR product would not have these two forms of plasmid.

DpnI recognize and cleave double stranded DNA which has methylated adenine residue on both strands in recognition site GATC. Plasmid purified from Dam⁺ strain was found to be hemi-methylated at certain site (Russell and Zinder 1987). Hemi-methylated DNA is cleaved by *DpnI* less efficiently (about sixty folds) compared to fully methylated DNA (Wang and Malcolm 1999; Robinson et al., 2001; Sambrook and Russell 2001; Liu and Naismith 2008). Hence, it would be hard to completely remove all the wild type templates if the wild type templates possessed some hemi-methylated DNA population.

In QCM method, during PCR process, the newly synthesized plasmid (unmethylated) may remain entangled to the single stranded wild type template (methylated), forming hemi-methylated heteroduplexes (Liu and Naismith 2008). These heteroduplexes could be resistant to *DpnI* digestion and get transformed into competent cells. The cells which took up these heteroduplexes could survive upon selective pressure of antibiotic since heteroduplexes carried the ampicillin resistance gene, resulting in recovery of parental plasmid (Wang and Malcolm 1999). Hence, one hour of post-PCR-*DpnI* digestion in QCM method may not be sufficient to remove all the parental templates.

Compared to QCM method, SPRINP method started with larger amount of wild type template. Hence, overnight *DpnI* digestion of PCR product would be needed. Cooling to promote random annealing after mixing the two single-primer PCR reaction product in this method could be another factor that yielded hemi-methylated heteroduplexes (as shown in Appendix A). Since the starting parental template was in large amount and yet the amplification efficiency was low, there would be high chance that the single stranded PCR products annealed to the single stranded wild type templates.

5.1.5 Future Studies

There are many approaches that possibly could address many of the problems and questions brought up in this study. Since in total there were 112 colonies obtained using both QCM method and SPRINP method for all the desired

mutant constructs, while the screened colonies were only 43 colonies, there would still be some possibilities that other colonies contain the desired mutant constructs. Hence, more colonies could be picked and screened for relevant mutant.

Since it appeared that transformation efficiency did not increase as expected after 12-24 hours of fresh preparation which might be due to temperature variation during transformation immediately after transformation, the freshly competent cell could be stored directly at 4 °C and only be used after 12-24 hours. This may improve the transformation efficiency since it would cause lesser disturbances to cells. Apart from this, other transformation protocol which had been reported to achieve transformation efficiency of 10^7 - 10^9 cfu/ μ g like Hanahan Method (Sambrook and Russell 2001).

One of the main problems in this study was consistent recovery of wild type constructs instead of desired mutant construct. The plasmid template could be denatured first using denaturing solution (1 M NaOH/ 1 mM EDTA) for 15 minutes at 37 °C before proceeding to PCR. This denaturation process could destroy the transforming ability of wild-type plasmid template, thus reducing the background colonies which contain the wild type construct and therefore chances of recovering them (Du et al., 1995; Dorrell et al., 1996). Besides, it may improve the amplification efficiency as discussed earlier in Section 5.1.3.2.

In order to increase the amplification efficiency of the PCR, optimization of annealing temperature or touchdown PCR could be tried (Roux 2009). This allows more annealing event of mutagenic primer to the target site of the plasmid template, thus more primer extension and subsequent mutant amplification. To reduce the secondary structures that may inhibit annealing of primer to template, PCR additive BSA and DMSO could be added together into PCR (QCM method and SPRINP method) reaction, which would have better amplification efficiency compared to addition of DMSO only into the PCR reaction (Farell and Alexandre 2012).

If all the above approaches fail to generate desired mutant constructs, new primers with better annealing rate to the template or reduced self-annealing temperature (T_m) could be designed. The primers could be designed in a way that restriction enzyme cleavage sites are introduced near the target sequence, without changing the amino acid sequence via strategy like designed restriction endonuclease-assisted mutagenesis (DREAM) (Zhang et al., 2009). This would facilitate the mutant screening which allows more practical mutagenesis in terms of cost and time.

5.2 Generation of γ -syn Gene Silencing Constructs

5.2.1 Dual Digestion of Lentiviral Plasmid pLKO.1 TRC

To avoid DNA loss which may occur during intermediate gel purification process (Patel et al., 2012) that may contribute to low final DNA yield, simultaneous dual digestion of pLKO.1 TRC was performed instead of

sequential dual digestion. Following simultaneous digestion of pLKO.1 TRC with *Age*I and *Eco*RI and subsequent gel purification, a thick 7 kb band could be observed on gel as shown in Figure 4.10.

Absence of other band of different size on the gel as shown on Lane 1 in Figure 4.10 and Lane 4 in Figure 4.12 indicated that the gel purification process was clean. This was further supported by absence of colony on negative control plate for vector self-ligation after transformation. This eliminated the possibility of presence of trace amount of incomplete dual-digested plasmid vector in the gel purification product for non-stuffer pLKO.1 which could not be detected on gel.

5.2.2 Suboptimal Efficiency of shRNA Oligonucleotides Annealing

The oligonucleotides annealing efficiency for the three shRNA constructs was predicted to be suboptimal since the upper band on Lanes 2, 3 and 4 appeared to be thinner than the respective lower band on the same lane.

After heating the oligonucleotides mixtures to 95 °C for 4 minutes, all the secondary structures of the single-stranded oligonucleotides (forward and reverse) would be melted. Slow cooling after heat denaturation was important to ensure proper annealing between forward oligonucleotides and reverse oligonucleotides. Since, there were sense and anti-sense sequences which were completely matched within single-stranded oligonucleotide, rapid cooling after denaturation may facilitate intra-molecular annealing (form self-loop

migrating as lower band on all the lanes in Figure 4.11), resulting in inefficient inter-molecular oligonucleotides annealing (form dimer migrating as upper band on all the lanes in Figure 4.11). Hence, in order to allow slower cooling process in this step, the beaker containing water bath for incubation of oligonucleotides mixtures was not moved to bench top after heating, instead, left undisturbed on the tripod stand.

Oligonucleotides annealing would never be 100% efficient (Life Technologies Corporation n.d.). The efficiency could be affected by concentration of salt (Thermo Scientific 2009), oligonucleotides (Life Technologies Corporation n.d.) and the cooling rate (Thermo Scientific 2009). The single-stranded oligonucleotides used in this study had sense and anti-sense sequences, thus contributing to their strong hairpin potential. Hence, there is possibility that these oligonucleotides quickly self-annealed and thus could not form proper inter-molecular annealing with complementary oligonucleotides, leading to suboptimal oligonucleotides annealing efficiency.

5.2.3 Plasmid Instability

Multiple attempts of transformation of ligation products for all the three shRNA constructs into both competent DH5 α and JM109 failed to produce colonies except for the final attempt where few colonies were obtained. Subsequent minipreparation on the colonies produced plasmid with structural change. Since ligation of all the three shRNA constructs appeared to be successful with the mobility shift of ligation band compared to non-stuffer

pLKO.1 band as shown in Figure 4.13, plasmid instability was suspected to occur.

Plasmid instability often poses difficulties in cloning especially when a particular unstable sequence present in the vector or vector-insert assembly (Razin et al., 2001; Al-Allaf et al., 2005). Plasmid instability often causes reduced or inhibited growth of bacterial hosts, rearrangement of the plasmid structure and decrease in copy number which eventually leads to plasmid loss (Al-Allaf et al., 2012). DNA sequences like multiple direct repeats (Bichara et al., 2000; Chakiath and Esposito 2007), long inverted repeats intervened by short segment (Prats et al., 1985) and regions capable of inducing strong secondary structures (Godiska et al., 2010) are often associated with plasmid instability.

The backbone of lentiviral plasmid pLKO.1 TRC contains long terminal repeat (LTR) sequence which may lead to plasmid instability due to its tendency to be involved in homologous recombination events (Chakiath and Esposito 2007; Tolmachov et al., 2011; Al-Allaf et al., 2012). Although *recA*-host strain DH5 α and JM109 which would have reduced recombination events were used in this study, direct repeat sequence still could evoke DNA rearrangement in a RecA-independent manner (Oliveria et al., 2009). As a consequence of recombination events, plasmid deletion often occurs to remove the direct repeat sequence, which may produce smaller plasmid losing some important sequences (Chakiath and Esposito 2007). The sizes of the purified plasmids deduced from their linear form as shown on Lanes 1-3 in Figure 4.13

were approximately 5200 bp, which was much smaller than the expected size of dual digested pLKO.1 TRC (~7000 bp). Production of four bands instead of expected two bands after dual digestion of pLKO.1 TRC as shown on Lanes 4-6 in Figure 4.13 may indicate occurrence of homologous recombination events. This was further supported by failure in sequencing of the purified plasmid which may indicate loss of priming site on the plasmid for the pLKO.1 sequencing primer. It is possible that after recombination, the structure of plasmid changed or reduced but it still retained the ampicillin resistance gene, hence the transformed cells able to survive of ampicillin selection.

The annealed oligonucleotides for all the three γ -syn shRNA constructs to be cloned into non-stuffer pLKO.1 TRC are composed of complementary sense and anti-sense sequences separated by a short loop sequence. This region may form unusual hairpin-like or cruciform-like secondary structure in the ligated circular plasmid (Voineagu et al., 2008), which also could contribute to plasmid instability. Both hairpin and cruciform structures may block DNA replication in bacteria via replication fork stalling at these structures (Voineagu et al., 2008). Besides, cruciform-like DNA structures are also known to be susceptible to endonuclease which may result in nicking of plasmid in bacteria (Williams et al., 2009) and could be a source of genomic instability in human (Kurahashi et al., 2004). These might serve as the mechanism to slow down the plasmid propagation, resulting in maintenance plasmid instability. This may explain the failure in obtaining colony after several attempts of transformation in this study.

Another possible explanation for plasmid instability could be the presence of cryptic bacterial promoter within the eukaryotic annealed oligo sequence. There are a number of studies suggesting that eukaryotic sequences may be toxic to bacterial hosts via driving the expression of toxic RNA and polypeptides (Yike et al., 1996; Tolmachov et al., 2011) or toxic insert mediated transcriptional read-through (Brosius 1984). This may exert negative selective pressure on bacterial populations carrying the constructs, resulting in plasmid maintenance instability. At the same time, this might also trigger the homologous recombination events, resulting in deletion of the toxic eukaryotic region. The plasmid deletion mutants would have greater selective advantage as compared to the plasmid carrying toxic eukaryotic sequence, and hence it was difficult to recover the desired recombinant clones.

5.2.4 Future Studies

Since plasmid instability appeared to be the main problem encountered in this study, switching over to another cloning host which could give better plasmid stability would be necessary. *E. coli* Stb13 could be a solution since it was reported able to provide better plasmid stability in terms of structure and maintenance than DH5 α , TOP10, JM109 and Stb12 possibly due to *recA13* allele of the *recA* mutation and genes derived from *E. coli* B ancestor (Al-Allaf et al., 2012). Besides, reduced-genome strain of *E. coli* MDS42 could also be used. It was reported to have reduced plasmid recombination events due to loss of insertion sequence (IS) elements and may perform even better than Stb13 (Chakiath and Esposito 2007).

Carbenicillin which is a more stable analog of ampicillin could be used to replace ampicillin to exert the selective pressure. Carbenicillin is less heat- and pH-sensitive as well as less labile to β -lactamase action as compared to ampicillin. Hence, it may persist in the culture media for longer incubation period and thus allowing better plasmid segregational and maintenance stability especially in liquid culture media used for subsequent plasmid extraction (Al-Allaf et al., 2012).

Besides, the condition of oligonucleotides annealing reaction including the concentration of salt and oligonucleotides used could be optimized to further improve the annealing efficiency in future. This may enhance subsequent ligation efficiency and thus increase the chance of cloning success.

CHAPTER 6

CONCLUSIONS

The self-prepared chemical competent cells used in this study achieved competency of 2.417×10^6 cfu/ μ g plasmid which met the range of transformation efficiency sufficient for routine cloning purpose. However, the attempts to generate α -syn phosphorylation mutant constructs (S87A, S87D, S129A and S129D) using QCM and SPRINP method were unsuccessful of which could be due to inefficient amplification of mutant products. Besides, the attempts to generate γ -syn gene silencing constructs using shRNA cloning method were unsuccessful of which could be due to plasmid instability. Further work addressing to these problems could be performed in order to create these constructs. This study highlighted the limitations of both site-directed mutagenesis and shRNA cloning methods which often impede the progress of researches. It may serve as a reference for other researchers in terms of experimental design and troubleshooting process when performing these two methods in future.

REFERENCES

- Abeliovich, A. et al., 2000. Mice lacking alpha-synuclein display functional deficits in the nigrostriatal dopamine system. *Neuron*, 25, pp. 239-252.
- Addgene, 2006. *pLKO.1 - TRC Cloning Vector*. [Online] Available at: <http://www.addgene.org/tools/protocols/plko/> [Accessed: 16 February 2013].
- Ahmah, M. et al., 2007. γ -synuclein and the progression of cancer. *The FASEB Journal*, 21, pp. 3419-3430.
- Al-Allaf, F. A. et al., 2012. Remarkable stability of an instability-prone lentiviral vector plasmid in *Escherichia coli* Stbl3. *3 Biotech*, 3, pp. 61-70.
- Al-Allaf, F. A. et al., 2005. Coupled analysis of bacterial transformants and ligation mixture by duplex PCR enables detection of fatal instability of a nascent recombinant plasmid. *Journal of Biochemical and Biophysical Methods*, 64, pp. 142-146.
- Albani, D. et al., 2004. Protective effect of TAT-delivered alpha-synuclein: relevance of the C-terminal domain and involvement of HSP70. *The FASEB Journal*, 18, pp. 1713-1715.
- Allam, M. F., Del Castillo, A. S. and Navajas, R. F., 2005. Parkinson's disease risk factors: genetic, environmental, or both? *Neurological Research*, 27, pp. 206-208.
- Anderson, J. P. et al., 2006. Phosphorylation of Ser-129 is the dominant pathological modification of alpha synuclein in familial and sporadic Lewy body disease. *Journal of Biological Chemistry*, 281, pp. 29739-29752.
- Baba, M. et al., 1998. Aggregation of alpha-synuclein in Lewy bodies of sporadic Parkinson's disease and dementia with Lewy bodies. *The American Journal of Pathology*, 152, pp. 879-884.
- Bartel, D. P., 2004. MicroRNAs: genomics, biogenesis, mechanism and function. *Cell*, 116, pp. 281-297.
- Bartels, T., Choi, J. G. and Selkoe, D. J., 2011. α -Synuclein occurs physiologically as a helically folded tetramer that resists aggregation. *Nature*, 477, pp. 107-110.
- Bentwich, I. et al., 2005. Identification of hundreds of conserved and nonconserved human microRNAs. *Nature Genetics*, 37, pp. 766-770.
- Betts, M. J. and Russell, R. B., 2003. Amino acid properties and consequences of substitutions. In: Barnes, M. R., and Gray, I. C. (eds.).

Bioinformatics for Geneticists. Chichester: John Wiley & Sons, Ltd, pp. 290-316.

- Bichara, M. et al., 2000. Mechanisms of dinucleotide repeat instability in *Escherichia coli*. *Genetics*, 154, pp. 533-542.
- Biere, A. L. et al., 2000. Parkinson's disease associated alpha-synuclein is more fibrillogenic than beta- and gamma-synuclein and cannot cross-seed its homologs. *The Journal for Biological Chemistry*, 275, pp. 34574-34579.
- Bisaglia, M. et al., 2010. α -synuclein overexpression increases dopamine toxicity in BE(2)-M17 cells. *BMC Neuroscience*, 11, doi: 10.1186/1471-2202-11-41.
- Braak, H. et al., 2003. Staging of brain pathology related to sporadic Parkinson's disease. *Neurobiology of Aging*, 24, pp. 197-211.
- Braak, H., Ghebremedhin, E. and Rüb, U., 2004. Stages in the development of Parkinson's disease-related pathology. *Cell and Tissue Research*, 318, pp. 121-134.
- Braithwaite, S. P. et al., 2012. Targeting phosphatases as the next generation of disease modifying therapeutics for Parkinson's disease. *Neurochemistry International*, 61, pp. 899-906.
- Braithwaite, S., Stock, J. B. and Mouradian, M. M., 2012. Alpha synuclein phosphorylation as a therapeutic target in Parkinson's disease. *Nature Reviews Neuroscience*, 23, pp. 191-198.
- Brosius, J., 1984. Toxicity of an overproduced foreign gene product in *Escherichia coli* and its use in plasmid vectors for the selection of transcription terminators. *Gene*, 27, pp. 161-172.
- Bruening, W. et al., 2000. Synucleins are expressed in the majority of breast and ovarian carcinomas and in preneoplastic lesions of the ovary. *Cancer*, 88, pp. 2154-2163.
- Buchman, V. L. et al., 1998. Persyn, a member of the synuclein family, has a distinct pattern of expression in the developing nervous system. *The Journal of Neuroscience*, 18, pp. 9335-9341.
- Bussell, R. J. and Eliezer, D., 2003. A structural and functional role for 11-mer repeats in α -synuclein and other exchangeable lipid binding proteins. *Journal of Molecular Biology*, 329, pp. 763-778.
- Carmell, M. A. and Hannon, G. J., 2004. RNase III enzymes and the initiation of gene silencing. *Nature Structural & Molecular Biology*, 11, pp. 214-218.

- Chakiath, C. S. and Esposito, D., 2007. Improved recombinational stability of lentiviral expression vectors using reduced-genome *Escherichia coli*. *Biotechniques*, 43, pp. 466-470.
- Chandra, S. et al., 2005. Alpha-synuclein cooperates with CSPalpha in preventing neurodegeneration. *Cell*, 123, pp. 383–396.
- Chau, K. Y. et al., 2009. Relationship between alpha synuclein phosphorylation, proteosomal inhibition and cell death: relevance to Parkinson's disease pathogenesis. *Journal of Neurochemistry*, 110, pp. 1005-1013.
- Chen, X. et al., 1995. The human NACP/alpha-synuclein gene: chromosome assignment to 4q21.3-q22 and TaqI RFLP analysis. *Genomics*, 26, pp. 425-427.
- Cheng, F., Vivacqua, G. and Yu, S., 2010. The role of alpha-synuclein in neurotransmission and synaptic plasticity. *Journal of Chemical Neuroanatomy*, 42, pp. 242-248.
- Chen, J. et al., 2012. Neural protein gamma-synuclein interacting with androgen receptor promotes human prostate cancer progression. *BMC Cancer*, 12, doi: 10.1186/1471-2407-12-593
- Chen, L. and Feany, M., 2005. Alpha synuclein phosphorylation controls neurotoxicity and inclusion formation in a *Drosophila* model of Parkinson disease. *Nature Reviews Neuroscience*, 8, pp. 657-663.
- Choong, C. J., 2011. *Investigation of the dual cyto-toxic/-protective roles of α -synuclein in human neuroblastoma, SH-SY5Y and human melanoma, SK-MEL28 cells*. MSc Thesis, Universiti Tunku Abdul Rahman, Malaysia.
- Clayton, D. and George, J., 1998. The synucleins: a family of proteins involved in synaptic function, plasticity, neurodegeneration and disease. *Trends in Neuroscience*, 21, pp. 249-254.
- Crowther, R. et al., 1998. Synthetic filaments assembled from C-terminally truncated alpha-synuclein. *FEBS Letters*, 436, pp. 309-312.
- Cullen, B. R., 2004. Transcription and processing of human microRNA precursors. *Molecular Cell*, 16, pp. 861-865.
- Daubner, S. C., Le, T. and Wang, S., 2011. Tyrosine hydroxylase and regulation of dopamine synthesis. *Archives of Biochemistry and Biophysics*, 508, pp. 1-12.
- Davidson, W. et al., 1998. Stabilization of alpha-synuclein secondary structure upon binding to synthetic membranes. *The Journal of Biological Chemistry*, 273, pp. 9443-9449.

- Davie, C. A., 2008. A review of Parkinson's disease. *British Medical Bulletin*, 86, pp. 109-127.
- Dorrell, N. et al., 1996. Improved efficiency of inverse PCR mutagenesis. *BioTechniques*, 21, pp. 604-608.
- Du, Z., Regier, D. A. and Desrosiers, R. C., 1995. Improved recombination PCR mutagenesis procedure that uses alkaline-denatured plasmid template. *BioTechniques*, 18, pp. 376-378.
- Edelheit, O., Hanukoglu, A. and Hanukoglu, I., 2009. Simple and efficient site-directed mutagenesis using two single-primer reactions in parallel to generate mutants for protein structure-function studies. *BMC Biotechnology*, 9, doi: 10.1186/1472-6750-9-61.
- El-Agnaf, O., Salem, S. and Paleologou, K., 2003. Alpha-synuclein implicated in Parkinson's disease is present in extracellular biological fluids, including human plasma. *The FASEB Journal*, 17, pp. 1945-1947.
- Ellis, C. et al., 2001. alpha-synuclein is phosphorylated by members of the Src family of protein-tyrosine kinases. *The Journal of Biological Chemistry*, 276, pp. 3879-3884.
- Fang, D., 2004. Attempts to use PCR site-directed mutagenesis to create a non-functional rop gene in the plasmid pBR322. *Journal of Experimental Microbiology and Immunology*, 6, pp. 45-51.
- Farell, E. M. and Alexandre, G., 2012. Bovine serum albumin further enhances the effects of organic solvents on increased yield of polymerase chain reaction of GC-rich templates. *BMC Research Notes*, 5. doi: 10.1186/1756-0500-5-257.
- Fire, A. et al., 1998. Potent and specific genetic interference by double-stranded RNA in *Caenorhabditis elegans*. *Nature*, 391, pp. 806-811.
- Fujiwara, H. et al., 2002. α -synuclein is phosphorylated in synucleinopathy lesions. *Nature Cell Biology*, 4, pp. 160 - 164.
- Galvin, J. E. et al., 1999. Axon pathology in Parkinson's disease and Lewy body dementia hippocampus contains α -, β -, and γ -synuclein. *Proceedings of the National Academy of Sciences of the United States of America*, 96, pp. 13450-13455..
- Gaugler, M. et al., 2012. Nigrostriatal overabundance of alpha-synuclein leads to decreased vesicle density and deficits in dopamine release that correlate with reduced motor activity. *Acta Neuropathologica*, 125, pp. 653-669.
- George, J. M., 2001. The synucleins. *Genome Biology*, 3, pp. 3002.1-3002.6.

- Godiska, R. et al., 2010. Linear plasmid vector for cloning of repetitive or unstable sequences in *Escherichia coli*. *Nucleic Acid Research*, 38, doi: 10.1093/nar/gkp1181.
- Goldsmith, M. et al., 2007. Avoiding and controlling double transformation artifacts. *Protein Engineering, Design & Selection*, 20, pp. 315-318.
- Gonzalez-Alegre, P. and Paulson, H. L., 2007. Technology insight: therapeutic RNA interference - how far from the neurology clinic?. *Nature Clinical Practice Neurology*, 3, pp. 394-404.
- Gorbatyuk, O. S. et al., 2007. The phosphorylation state of Ser-129 in human alpha synuclein determines neurodegeneration. *Proceedings of the National Academy of Sciences of the United States of America*, 105, pp. 763-768.
- Guttmacher, A. E. and Collins, F. S., 2003. Alzheimer's disease and Parkinson's disease. *The New England Journal of Medicine*, 348, pp. 1356-1364.
- Hanahan, D. and Weinberg, R. A., 2000. The hallmarks of cancer. *Cell*, 100, pp. 57-70.
- Han, S. et al., 2012. SNCG gene silencing in gallbladder cancer cells inhibits key tumorigenic activities. *Frontiers in Bioscience*, 1, pp. 1589-1598.
- Hashimoto, M., Hsu, L. and Sisk, A., 1998. Human recombinant NACP/alpha-synuclein is aggregated and fibrillated in vitro: Relevance for Lewy body disease. *Brain Research*, 799, pp. 301-306.
- Inglis, K. et al., 2009. Polo-like kinase 2 (PLK2) phosphorylates alpha-synuclein at serine 129 in central nervous system. *The Journal of Biological Chemistry*, 284, pp. 2598-2602.
- Invitrogen, n.d. *Generating the Double-Stranded Oligo* [Online]. Available at: https://rnaidesigner.invitrogen.com/rnaiexpress/dsOligo_miRNA.pdf [Accessed: 15 December 2013].
- Invitrogen, 2007. *Meet all your transformation needs here - efficiency, genotype, and packaging options* [Online]. Available at: http://www.invitrogen.com/etc/medialib/en/filelibrary/pdf/Brochures.Par.7806.File.dat/B-069876-CompCellBro_LRF.pdf [Accessed: 7 February 2013].
- Invitrogen, 2013. *pcDNA™3.1 Directional TOPO® Expression Kit* [Online]. Available at: <https://products.invitrogen.com/ivgn/product/K490001> [Accessed: 2 February 2013].
- Jakes, R., Spillantini, M. G. and Goedert, M., 1994. Identification of two distinct synucleins from human brain. *FEBS Letters*, 345, pp. 27-32.

- Ji, H. et al., 1997. Identification of a breast cancer-specific gene, BCSG1, by direct differential cDNA sequencing. *Human Genome Sciences*, 57, pp. 759-764.
- Kahle, P., 2008. α -synucleinopathy models and human neuropathology: Similarities and differences. *Acta Neuropathologica*, 115, pp. 87-95.
- Kanda, S. et al., 2000. Enhanced vulnerability to oxidative stress by alpha-synuclein mutations and C-terminal truncation. *Neuroscience*, 97, pp. 279–284.
- Kim, T., Paik, S. and Yang, C., 2002. Structural and functional implications of C-terminal regions of alpha-synuclein. *Biochemistry*, 41, pp. 13782-13790.
- Kokubo, Y. et al., 2012. α -synuclein pathology in the Amyotrophic Lateral Sclerosis/ Parkinsonism dementia complex in the Kii Peninsula, Japan. *Journal of Neuropathology & Experimental Neurology*, 71, pp. 625-630.
- Kordower, J. et al., 2008. Lewy-body like pathology in long term embryonic nigral transplants in Parkinson's disease. *Nature Medicine*, 14, pp. 504-506.
- Kramer, M. L. and Schulz-Schaeffer, W. J., 2007. Presynaptic α -Synuclein aggregates, not Lewy bodies, cause neurodegeneration in dementia with lewy bodies. *The Journal of Neuroscience*, 27, pp. 1405-1410.
- Kruger, R., 2004. *Parkinson disease, genetic types* [Online]. Available at: <http://www.orpha.net/data/patho/GB/uk-Parkinson.pdf> [Accessed: 4 July 2012].
- Kurahashi, H. et al., 2004. Cruciform DNA structure underlies the etiology for palindrome-mediated human chromosomal translocation. *The Journal of Biological Chemistry*, 279, pp. 35377-35383.
- Laible, M. and Boonrod, K., 2009. Homemade site directed mutagenesis of whole plasmids. *Journal of Visualized Experiments*, 27, doi: 10.3791/1135.
- Lavedan, C., 1998. The synuclein family. *Genome Research*, 8, pp. 871-880.
- Lee, K. W. et al., 2011. Enhanced phosphatase activity attenuates α -synucleinopathy in mouse model. *Neurobiology of Disease*, 31, pp. 6963-6971.
- Leger, J. et al. 1997. Conversion of serine to aspartate imitates phosphorylation-induced changes in the structure and function of microtubule-associated protein Tau. *The Journal of Biological Chemistry*, 272, pp. 8441-8446.

- Li, J. et al., 2008. Lewy bodies in grafted neurons in subjects with Parkinson's disease suggest host-to-graft disease propagation. *Nature Medicine*, 14, pp. 501-503.
- Li, M. J. et al., 2010. The reciprocal regulation of gamma-synuclein and Insulin-like Growth Factor-1 (IGF-1) receptor expression creates a circuit that modulates IGF-1 signalling. *The Journal of Biological Chemistry*, 285, pp.30480-30488.
- Ling, M. M. and Robinson, B. H., 1997. Approaches to DNA mutagenesis: An overview. *Analytical Biochemistry*, 254, pp. 157-178.
- Liu, H. et al., 2005. Loss of epigenetic control of Synuclein- γ gene as a molecular indicator of metastasis in a wide range of human cancers. *Cancer Research*, 65, pp. 7635-7643.
- Liu, H. and Naismith, J. H., 2008. An efficient one-step site-directed deletion, insertion, single and multiple-site plasmid mutagenesis protocol. *BMC Biotechnology*, 8. doi:10.1186/1472-6750-8-91.
- Li, W. et al., 2005. Aggregation promoting C-terminal truncation of alpha-synuclein is a normal cellular process and is enhanced by the familial Parkinson's disease-linked mutations. *Proceedings of the National Academy of Sciences of the United States of America*, 2, pp. 2162-2167.
- Lou, H. et al., 2010. Serine 129 phosphorylation reduces the ability of alpha-synuclein to regulate tyrosine hydroxylase and protein phosphatase 2A in vitro and in vivo. *The Journal of Biological Chemistry*, 285, pp. 17648-17661.
- McCormack, A. L., Mak, S. K. and Monte, D. D., 2012. Increased α -synuclein phosphorylation and nitration in the aging primate substantia nigra. *Cell Death and Disease*, 3, doi: 10.1038/cddis.2012.50.
- McFarland, N. R. et al., 2009. Alpha-synuclein S129 phosphorylation mutants do not alter nigrostriatal toxicity in a rat model of Parkinson Disease. *Journal of Neuropathology and Experimental Neurology*, 68, pp. 515-524.
- McIntyre, G. J. and Fanning, G. C., 2006. Design and cloning strategies for constructing shRNA expression vectors. *BMC Biotechnology*, 6, doi:10.1186/1472-6750-6-1.
- Meister, G. et al., 2004. Human Argonaute 2 mediates RNA cleavage targeted by miRNAs and siRNAs. *Molecular Cell*, 15, pp. 185-197.
- Moffat, J. et al., 2006. A lentiviral RNAi library for human and mouse genes applied to an arrayed viral high-content screen. *Cell*, 124, pp. 1283-1298.
- Mukaetova-Ladinska, E. et al., 2009. Lewy body variant of Alzheimer's disease: selective neocortical loss of t-SNARE proteins and loss of

- MAP2 and alpha-synuclein in medial temporal lobe. *ScientificWorld Journal*, 9, pp. 1463-1475.
- Muntane, G., Ferrer, I. and Martinez-vincente, M., 2012. α -synuclein phosphorylation and truncation are normal events in the adult human brain. *Neuroscience*, 200, pp. 107-119.
- Nemani, V. et al., 2010. Increased expression of alpha-synuclein reduces neurotransmitter release by inhibiting synaptic vesicle reclustering after endocytosis. *Neuron*, 65, pp. 66-79.
- Neumann, M. et al., 2000. Alpha-synuclein accumulation in a case of neurodegeneration with brain iron accumulation type 1 (NBIA-1, formerly Hallervorden-Spatz syndrome) with widespread cortical and brainstem-type Lewy bodies. *Acta Neuropathologica*, 100, pp. 568-574.
- New England Biolabs, n.d. *DNA polymerase strand displacement activity* [Online]. Available at: <https://www.neb.com/products/polymerases-and-amplification-technologies/polymerases-and-amplification-technologies/dna-polymerase-strand-displacement-activity> [Accessed: 1 March 2013].
- Nikolova, D. and Toncheva, D., 2008. RNA interference - regulations and application in oncology. *Journal of Cancer Molecules*, 4, pp. 67-77.
- Ninkina, N. N. et al., 1998. Organization, expression and polymorphism of the human persyn gene. *Human Molecular Genetics*, 7, pp. 1417-1424.
- Okochi, M. et al., 2000. Constitutive phosphorylation of the Parkinson's disease associated alpha-synuclein. *The Journal of Biological Chemistry*, 275, pp. 390-397.
- Oliveria, P. H. et al., 2009. Structural instability of plasmid biopharmaceuticals: challenges and implications. *Trends in Biotechnology*, 27, pp. 503-511.
- Oueslati, A. et al., 2012. Mimicking phosphorylation at serine 87 inhibits the aggregation of human α -synuclein and protects against its toxicity in a rate model of Parkinson's disease. *Neurobiology of Disease*, 32, pp. 1536-1544.
- Paddison, P. J. et al., 2002. Short hairpin RNAs (shRNAs) induce sequence-specific silencing in mammalian cells. *Cold Spring Harbor Laboratory Press*, 16, pp. 948-958.
- Paleologou, K. E. et al., 2010. Phosphorylation at S87 is enhanced in synucleinopathies, inhibits α -synuclein oligomerization and influences synuclein-membrane interactions. *The Journal of Neuroscience*, 30, pp. 3184-3198.
- Paleologou, K. E. et al., 2008. Phosphorylation at ser-129 but not phosphomimics S129E/D inhibits the fibrillation of α -synuclein. *The Journal of Biological Chemistry*, 283, pp. 16895-16905.

- Patel, A. et al., 2012. Creation and validation of a ligation-independent cloning (LIC) retroviral vector for stable gene transduction in mammalian cells. *BMC Biotechnology*, 12, doi: 10.1186/1472-6750-12-3.
- Perez, R. G. et al., 2002. A role for alpha-synuclein in the regulation of dopamine biosynthesis. *The Journal of Neuroscience*, 22, pp. 3090-3099.
- Prats, H. et al., 1985. A plasmid vector allowing positive selection of recombinant plasmids in *Streptococcus pneumoniae*. *Gene*, 39, pp. 41-48.
- Primrose, S. B. and Twyman, R., 2006. *Principles of Gene Manipulation and Genomics*. 7th ed. Carlton: Wiley-Blackwell.
- Pochapsky, T., 2012, *Protein structure and Parkinson's Disease* [Online]. Available at http://www.bio.brandeis.edu/pochapskylab/Pochapsky_Lab/Parkinsons.html [Accessed: 31 March 2013].
- Qing, H. et al., 2009. Lrrk2 phosphorylates alpha synuclein at serine 129: Parkinson disease implications. *Biochemical and Biophysical Research Communications*, 387, pp. 149-152.
- Razin, S. et al., 2001. Non-clonability correlates with genomic instability: a case study of a unique DNA region. *Journal of Molecular Biology*, 307, pp. 481-486.
- Reece, R. J., 2004. *Analysis of Genes and Genomes*. Chichester: John Wiley & Sons.
- Robinson, D., Walsh, P. R. and Bonventre, J. A., 2001. Restriction Endonucleases. In: Gerstein, A. S. (eds.). *Molecular Biology Problem Solver: A Laboratory Guide*. New York: Wiley-Liss Inc.
- Roux, K. H., 2009. Optimization and Troubleshooting in PCR. *Cold Spring Harbor Protocols*, 4, doi:10.1101/pdb.ip66.
- Russell, D. W. and Zinder, N. D., 1987. Hemimethylation prevents DNA replication in *E. coli*. *Cell*, 50, pp. 1071-1079.
- Saha, A. R. et al., 2003. Parkinson's disease a-synuclein mutations exhibit defective axonal transport in cultured neurons. *Journal of Cell Science*, 117, pp. 1017-1024.
- Sakamoto, M. et al., 2009. Contribution of endogenous G-protein coupled receptor kinases to Ser129 phosphorylation of alpha-synuclein in HEK293 cells. *Biochemical and Biophysical Research Communications*, 384, pp. 378-382.
- Sambrook, J. and Russell, D., 2001. *Molecular Cloning A Laboratory Manual*. 3rd ed. New York: Cold Spring Harbor Laboratory Press.

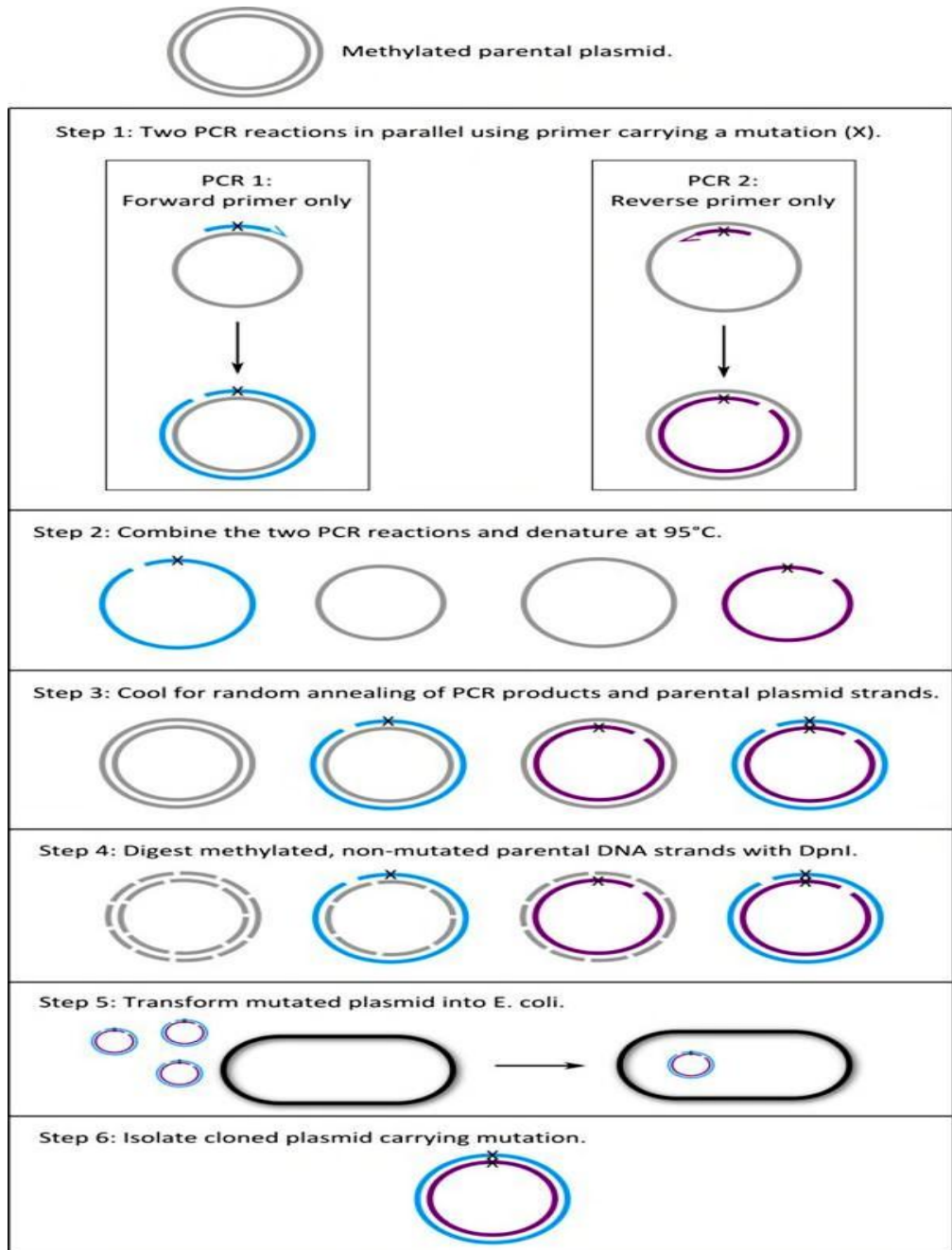
- Sato, H. et al., 2011. Authentically phosphorylated α -synuclein at Ser129 accelerates neurodegeneration in a rat model of familial Parkinson's disease. *Neurobiology of Disease*, 31, pp. 16884-16894.
- Shen, P. H. et al., 2011. SNCG shRNA suppressed breast cancer cell xenograft formation and growth in nude mice. *Chinese Medical Journal*, 124, pp. 1524-1528.
- Sigma-Aldrich, n.d. *Optimizing qPCR* [Online]. Available at: http://www.sigmaaldrich.com/etc/medialib/docs/SAJ/Brochure/1/j_qpcr_techguide06.Par.0001.File.tmp/j_qpcr_techguide06.pdf [Accessed: 31 January 2013].
- Singh, M. et al., 2010. Plasmid DNA transformation in *Escherichia coli*: Effect of heat shock temperature, duration, and cold incubation of CaCl₂ treated cells. *International Journal of Biotechnology and Biochemistry*, 6, pp. 561-568.
- Smith, W. W. et al., 2005. Alpha synuclein phosphorylation enhances eosinophilic cytoplasmic inclusion formation in SH-SY5Y cells. *The Journal of Neuroscience*, 25, pp. 5544-5552.
- Specht, G. et al., 2005. Subcellular localisation of recombinant alpha- and gamma-synuclein. *Molecular and Cellular Neuroscience*, 28, pp. 326-334.
- Spillantini, M. G., Divane, A. and Goedert, M., 1995. Assignment of human alpha-synuclein (SNCA) and beta-synuclein (SNCB) genes to chromosomes 4q21 and 5q35. *Genomics*, 27, pp. 379-381.
- Stefanis, L., 2012. α -synuclein in Parkinson's disease. *Cold Spring Harbor Perspectives in Medicine*, 2, doi:10.1101/cshperspect.a009399.
- Sundquist, T. and Doers, M., 1998. Optimized cloning with T vectors. *Promega Notes*, 68, pp. 31.
- Sung, J. et al., 2005. Proteolytic cleavage of extracellular secreted α -synuclein via matrix metalloproteinases. *The Journal of Biological Chemistry*, 280, pp. 25216-25224.
- Surgucheva, I. et al., 2003. Effect of gamma-synuclein overexpression on matrix metalloproteinases in retinoblastoma Y79 cells. *Archives of Biochemistry and Biophysics*, 410, pp. 167-176.
- Surgucheva, I. et al., 2002. Synuclein in glaucoma: implication of gamma synuclein in glaucomatous alterations in the optic nerve. *Journal of Neuroscience Research*, 68, pp. 97-106.
- Surgucheva, I., Sharov, V. S. and Surguchov, A., 2012. γ -synuclein: Seeding of α -synuclein aggregation and transmission between cells. *Biochemistry*, 51, pp. 4743-4754.

- Surgucheva, I., Shestopalov, V. I. and Surguchov, A., 2008. Effect of γ -synuclein silencing on apoptotic pathways in retinal ganglion cells. *The Journal of Biological Chemistry*, 283, pp. 36377-36385.
- Thermo Scientific, 2009. *Anneal complementary pairs of oligonucleotide* [Online]. Available at: <http://www.piercenet.com/files/TR0045-Anneal-oligos.pdf> [Accessed: 3 February 2013].
- Thermo Scientific, n.d. *Assessment of Nucleic Acid Purity* [Online]. Available at: <http://www.nanodrop.com/Library/T042-NanoDrop-Spectrophotometers-Nucleic-Acid-Purity-Ratios.pdf> [Accessed: 20 November 2012].
- Tokuda, T. et al., 2006. Decreased alpha-synuclein in cerebrospinal fluid of aged individuals and subjects with Parkinson's disease. *Biochemical and Biophysical Research Communications*, 349, pp. 162-166.
- Tolmachov, O. E., Tolmachova, T. and Al-Allaf, F. A., 2011. Designing Lentiviral Gene Vector. In: Xu, K. (ed.) *Viral Gene Therapy*. ISBN: 978-953-307-539-6, InTech, doi: 10.5772/17361. Available at: <http://www.intechopen.com/books/viral-gene-therapy/designing-lentiviral-gene-vectors>.
- Tong, J. et al., 2010. Brain α -synuclein accumulation in multiple system atrophy, Parkinson's disease and progressive supranuclear palsy: a comparative investigation. *Brain*, 133, pp. 172-188.
- Tu, Z. M. et al., 2005. An improved system for competent cell preparation and high efficiency plasmid transformation using different *Escherichia coli* strains. *Electronic Journal of Biotechnology*, 8, pp. 114-120.
- Uversky, V. and Fink, A. L., 2002. Amino acid determinants of α -synuclein aggregation: putting together pieces of puzzles. *FEBS Letters*, 522, pp. 9-13.
- Valtierra, S., 2008. α -synuclein phosphorylation and nitration in Parkinson's disease. *Eukaryon*, 4, pp. 90-94.
- Voineagu, I. et al., 2008. Replication stalling at unstable inverted repeats: Interplay between DNA hairpins and fork stabilizing proteins. *Proceeding of the National Academy of Sciences of the United States of America*, 105, pp. 9936-9941.
- Wang, W. and Malcolm, B. A., 1999. Two-Stage PCR protocol allowing introduction of multiple mutations, deletions and insertions using QuickChange Site-directed Mutagenesis. *Biotechniques*, 26, pp. 680-682.
- Watson, J. et al., 2009. Alterations in corticostriatal synaptic plasticity in mice overexpressing human alpha-synuclein. *Neuroscience*, 159, pp. 501-513.

- Williams, J. A., Carnes, A. E. and Hodgson, C. P., 2009. Plasmid DNA vaccine vector design: impact on efficacy, safety and upstream production. *Biotechnology Advances*, 27, pp. 353-370.
- Wu, B. et al., 2009. Phosphorylation of alpha-synuclein upregulates tyrosine hydroxylase activity in MN9D cells. *Acta Histochemica*, 113, pp. 32-35.
- Wu, K. et al., 2003. Stage-specific expression of breast cancer-specific gene. *Cancer Epidemiology, Biomarkers & Prevention*, 12, pp. 920-925.
- Yang, M. et al., 2010. Dynamic transport and localization of alpha synuclein in primary hippocampal neurons. *Molecular Neurodegeneration*, 5, doi:10.1186/1750-1326-5-9.
- Yike, I. et al., 1996. *Escherichia coli* of cytoplasmic portions of the cystic fibrosis transmembrane conductance regulator: apparent bacterial toxicity of peptides containing R-domain sequences. *Protein Expression and Purification*, 7, pp. 45-50.
- Zawaira, A. et al., 2012. A discussion of molecular biology methods for protein engineering. *Molecular Biotechnology*, 51, pp. 67-102.
- Zhang, B. Z. et al., 2009. An easy-to-use site-directed mutagenesis method with a designed restriction site for convenient and reliable mutant screening. *Journal of Zhejiang University*, 10, pp. 479-482.
- Zhang, H. et al., 2011. Role of gamma-synuclein in microtubule regulation. *Experimental Cell Research*, 317, pp. 1330-1339.
- Zhao, W. et al., 2006. Abnormal activation of the synuclein-gamma gene in hepatocellular carcinomas by epigenetic alteration. *International Journal of Oncology*, 28, pp. 1081-1088.
- Zheng, L., Baumann, U. and Reymond, J.-L., 2004. An efficient one-step site-directed and site-saturation mutagenesis protocol. *Nucleic Acids Research*, 32, doi: 10.1093/nar/gnh110.
- Zhou, F. et al., 2010. Application of short hairpin RNAs (shRNAs) to study gene function in mammalian systems. *African Journal of Biotechnology*, 9, pp. 9086-9091.
- Zhou, Y., Inaba, S. and Liu, J., 2006. Inhibition of synuclein-gamma expression increases the sensitivity of breast cancer cells to paclitaxel treatment. *International Journal of Oncology*, 29, pp. 289-295.

Appendix A

Schematic diagrams for Single Primer Reaction in Parallel (SPRINP) method



Adapted from Edelheit et al. (2009).

Appendix B

Homo-dimer analysis of primers for α -syn phosphorylation mutant constructs

for using online oligonucleotides analysis tool OligoAnalyzer 3.1

Delta G -7.05 kcal/mole

Base Pairs 4

```
5' GTGGAGGGAGCAGGGGCGATTGCAGCAGCCAC
      : ::  |||  :: :
3' CACCGACGACGTTAGCGGGGACGAGGGAGGTG
```

Primer for S87A phosphorylation mutant construct

Delta G -7.05 kcal/mole

Base Pairs 4

```
5' GGAGGGAGCAGGGGACATTGCAGCAGCC
      :  |||  :
3' CCGACGACGTTACAGGGGACGAGGGAGG
```

Primer for S87D phosphorylation mutant construct

Delta G -7.81 kcal/mole

Base Pairs 4

```
5' GAGGCTTATGAAATGCCTGCGGAGGAAGGGTATCAAGAC
      ||| : : : : :
3' CAGAACTATGGGAAGGAGGCGTCCGTAAAGTATTCGGAG
```

Primer for S129A phosphorylation mutant construct

Delta G -6.21 kcal/mole

Base Pairs 3

```
5' GGCTTATGAAATGCCTGATGAGGAAGGGTATCAAG
      || : : : : :
3' GAACTATGGGAAGGAGTAGTCCGTAAAGTATTCGG
```

Primer for S129D phosphorylation mutant construct